NASA TECHNICAL NOTE

NASA TN D-3565

NASA TN D-3565

VALIDATION OF A RESEARCH SIMULATOR FOR INVESTIGATING JET TRANSPORT HANDLING QUALITIES AND AIRWORTHINESS CRITERIA DURING TAKEOFF

by Charles T. Jackson, Jr., and C. Thomas Snyder

Ames Research Center
Moffett Field, Calif.

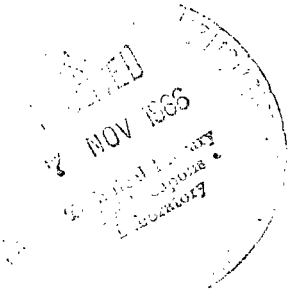

NATIONAL AERONAUTICS AND SPACE ADMINISTRATION • WASHINGTON, D. C. • OCTOBER 1966

NASA TN D-3565

VALIDATION OF A RESEARCH SIMULATOR FOR INVESTIGATING JET TRANSPORT HANDLING QUALITIES AND AIRWORTHINESS CRITERIA DURING TAKEOFF

By Charles T. Jackson, Jr., and C. Thomas Snyder

Ames Research Center
Moffett Field, Calif.

NATIONAL AERONAUTICS AND SPACE ADMINISTRATION

For sale by the Clearinghouse for Federal Scientific and Technical Information
Springfield, Virginia 22151 – Price $2.50

TABLE OF CONTENTS

VALIDATION OF A RESEARCH SIMULATOR FOR INVESTIGATING JET TRANSPORT HANDLING QUALITIES AND AIRWORTHINESS CRITERIA DURING TAKEOFF

By Charles T. Jackson, Jr., and C. Thomas Snyder
Ames Research Center

SUMMARY

A fixed-base simulator with an external visual display was used to simulate a current turbojet transport throughout the range of certification takeoff maneuvers. The resulting data and pilot opinions were then compared to the actual flight test data for that aircraft. Correlation was achieved between these data, and participating pilots agreed as to the duplication of the performance and "feel" of the aircraft. The simulator development program indicated the requirements for (1) valid aerodynamic data, in particular, ground effect data, (2) lateral motion of the cockpit for tests involving asymmetric thrust where the recognition of engine failure is important, and (3) good response of the simulator visual display.

INTRODUCTION

Civil aircraft must meet airworthiness standards set by the Federal Aviation Agency (FAA). As new types of aircraft are designed, new certification tests (refs. 1 and 2) may be required to insure standards of safety, reliability and repeatability that protect the traveling public and yet are technically attainable. Supersonic transports will have unique characteristics and require supplementary standards. Piloted simulators, which have proven to be useful for the study of general handling qualities (refs. 3 to 5), would appear to be useful in defining the relative importance or applicability of various certification criteria and to enable study of the significant variables. The simulator could be used as a tool to guide flight testing and for exposing possible areas of difficulty during the design and development of SST aircraft. In later stages of SST development the simulator would be used to familiarize flight crews and to provide design information for SST operational flight trainers (ref. 6).

A simulator intended for investigating the flying qualities of an aircraft still in the design stage should first be validated using a well-documented airplane as a reference. In this way, inadequacies and programming errors may be located and corrected. To establish the validity of the simulator for the above application, and to determine the particular features that should be included in the simulator, a program was conducted at the Ames Research Center, in which the maneuvers flown by a current subsonic turbojet transport to show compliance with existing regulations were also "flown" on

the simulator, and the results were compared. The present report describes the method and results of this validation with maneuvers restricted to the takeoff regime.

Acknowledgement is made to the Federal Aviation Agency and, in particular, to Mr. J. J. Tymczyszyn (Chief, West Coast SST Field Office) for their advice and assistance during the establishment of the program. Appreciation is due the Douglas Aircraft Company for the data and cooperation provided.

SYMBOLS

ANU,AND	airplane-nose up, airplane-nose down
a_X, a_Y, a_Z	accelerations in wind axes (positive forward, right and down, respectively), ft/sec^2
a.c.	aerodynamic center
b	wing span, ft
b_{mg}, b_{ng}	damping constant of main gear, nose gear, respectively, lb/ft/sec
C_D	drag coefficient, $\frac{\text{drag force}}{q_o S}$
C_L	lift coefficient, $\frac{\text{lift force}}{q_o S}$
C_{L_∞}	lift coefficient out of ground effect
C_l	rolling-moment coefficient, $\frac{\text{rolling moment}}{q_o S b}$
C_m	pitching-moment coefficient, $\frac{\text{pitching moment}}{q_o S \bar{c}}$
C_{m_o}	C_m at zero angle of attack
C_n	yawing-moment coefficient, $\frac{\text{yawing moment}}{q_o S b}$
C_Y	side-force coefficient, $\frac{\text{side force}}{q_o S}$
$C_{1/2}$	cycles to damp to half-amplitude
$\bar{c}$	wing mean aerodynamic chord, ft
c.g.	center of gravity
d	perpendicular distance thrust line is below c.g., ft
D	aerodynamic drag, lb

F_L, F_R, F_{ng}	normal force on left, right, and nose gear, respectively (compression, positive), lb
F_s	landing gear side force, lb
g	acceleration due to gravity, 32.2 ft/sec^2
$( )_{GE}$	ground effect
h	c.g. height above reference level -- zero when airplane is in level attitude with shock struts fully extended and main wheels just touching runway (up, positive), ft
h_o	nominal height of c.g. above ground level in taxi attitude, ft
h_{op}	height of pilot's eyes above ground when $h = \theta = 0$, ft
h_{ot}	height of tail (skid) above ground when $h = \theta = 0$, ft
h_p	height of pilot's eyes above ground level, ft
h_{tc}	vertical clearance between tail skid and runway, ft
i_H	horizontal stabilizer angle of incidence (AND, positive), radians
i_T	thrust angle of incidence with body X-axis (up, positive), radians
I_X, I_Y, I_Z	rolling, pitching, and yawing moments of inertia, respectively, slug-ft^2 (body axes)
K	engine thrust lapse with airspeed, lb/ft/sec
k_{ng}	nose gear strut spring constant, lb/ft
L	aerodynamic lift force, lb
$( )_{LG}$	landing gear
l_{cg}	x-distance c.g. forward of a.c., ft
l_{mg}	x-distance aerodynamic center forward of main gear, ft
l_{ng}	x-distance nose gear forward of a.c., ft
l_p	x-distance of pilot forward of nominal c.g. position, ft
l_t	x-distance of tail skid aft of nominal c.g. position, ft
m	airplane mass, slugs
p	roll angular velocity (right roll, positive), radians/sec

q	pitch angular velocity (ANU, positive), radians/sec
q_o	dynamic pressure, $\rho \frac{V^2}{2}$, lb/ft^2
RPS	rudder pedal steering
RTO	rejected takeoff (refused takeoff)
r	yaw angular velocity (nose right, positive), radians/sec
S	wing reference area, ft^2
s	distance along ground track, ft
T	total thrust, lb
T_n	net thrust per engine, lb
T_{static}	static thrust per engine, lb
T_1, T_2, T_3, T_4	thrust from left outboard, left inboard, right inboard, and right outboard engines, respectively, lb
$T_{1/2}$	time to damp to half-amplitude, sec
V	equivalent airspeed, ft/sec unless otherwise indicated
V_{EF}	speed at which engine failure occurs, knots
V_{LOF}	speed at main gear lift-off, knots
V_{MC_A}	air minimum control speed, knots
V_{MC_G}	ground minimum control speed, knots
V_{MU}	minimum unstick speed, knots
V_R	speed at time of rotation control input, knots
$V_{s_{1g}}$	1g stall speed, knots
$V_{s_{min}}$	minimum stall speed, knots
V_1	takeoff decision speed, knots
$V_{1_{test}}$	modified V_1 for particular test, knots
V_2	takeoff safety speed, knots
W	gross weight, lb

y_{mg}	distance from fuselage plane of symmetry to main gear, ft
y_p	lateral displacement of pilot station normal to runway center line, ft
y_1, y_2	distance from fuselage plane of symmetry to outboard and inboard engines, respectively, ft
Z_L, Z_R, Z_{ng}	left, right, and nose gear strut compressions, respectively -- zero when fully extended, ft
α	angle of attack, radians
β	angle of sideslip (relative wind from right, positive), radians
γ	flight-path angle (climb, positive), radians and percent
δ_a	average aileron deflection (right aileron up, positive), radians
δ_e	elevator deflection (AND, positive), radians
δ_F	flap deflection, radians
δ_{mg}	main gear tracking angle (wheel-heading right of direction of gear translation, positive), radians
δ_{ng}	nose gear tracking angle (wheel-heading right of direction of gear translation, positive), radians
δ_{ngs}	nose gear steering angle (wheel-heading right of fuselage center line, positive), radians
δ_r	rudder deflection (trailing edge right, positive), radians
θ	pitch angle of airplane body axis relative to horizon (ANU, positive), radians
μ_b	coefficient of braking friction, $\frac{\text{braking force}}{\text{landing gear load}}$
μ_L, μ_R	sum of coefficients of rolling resistance and braking friction of left and right main gear, respectively
μ_r	coefficient of rolling resistance
μ_s	coefficient of tire side force (parallel to axle)
ρ	air density, slugs/ft^3
τ_e	engine first-order-response time constant, sec

τ_r rudder servo system first-order-response time constant, sec

φ angle of bank (right wing down, positive), radians

$\frac{|\varphi|}{|V_e|}$ roll angle to sideslip parameter, $\frac{57.3}{V}\frac{|\varphi|}{|\beta|}$, deg/ft/sec

ψ_i yaw angle (heading) of airplane relative to a reference direction (nose right, positive), radians

ψ_w azimuth angle of flight path (track) relative to a reference direction (right, positive), radians

$(\dot{})$ derivative with respect to time, $\frac{d}{dt}$

$C_{L_{i_H}} = \frac{\partial C_L}{\partial i_H}$ $C_{l_{\delta_r}} = \frac{\partial C_l}{\partial \delta_r}$ $C_{n_r} = \frac{\partial C_n}{\partial (rb/2V)}$

$C_{L_q} = \frac{\partial C_L}{\partial (q\bar{c}/2V)}$ $C_{m_{i_H}} = \frac{\partial C_m}{\partial i_H}$ $C_{n_\beta} = \frac{\partial C_n}{\partial \beta}$

$C_{L_{\delta_e}} = \frac{\partial C_L}{\partial \delta_e}$ $C_{m_q} = \frac{\partial C_m}{\partial (q\bar{c}/2V)}$ $C_{n_{\delta_a}} = \frac{\partial C_n}{\partial \delta_a}$

$C_{L_{\delta_F}} = \frac{\partial C_L}{\partial \delta_F}$ $C_{m_\alpha} = \frac{\partial C_m}{\partial \alpha}$ $C_{n_{\delta_r}} = \frac{\partial C_n}{\partial \delta_r}$

$C_{l_p} = \frac{\partial C_l}{\partial (pb/2V)}$ $C_{m_{\dot{\alpha}}} = \frac{\partial C_m}{\partial (\dot{\alpha}\bar{c}/2V)}$ $C_{Y_\beta} = \frac{\partial C_Y}{\partial \beta}$

$C_{l_r} = \frac{\partial C_l}{\partial (rb/2V)}$ $C_{m_{\delta_e}} = \frac{\partial C_m}{\partial \delta_e}$ $C_{Y_{\delta_r}} = \frac{\partial C_Y}{\partial \delta_r}$

$C_{l_\beta} = \frac{\partial C_l}{\partial \beta}$ $C_{m_{\delta_F}} = \frac{\partial C_m}{\partial \delta_F}$ $\mu_{s_{\delta_{mg}}} = \frac{\partial \mu_s}{\partial \delta_{mg}}$

$C_{l_{\delta_a}} = \frac{\partial C_l}{\partial \delta_a}$ $C_{n_p} = \frac{\partial C_n}{\partial (pb/2V)}$ $\mu_{s_{\delta_{ng}}} = \frac{\partial \mu_s}{\partial \delta_{ng}}$

TEST EQUIPMENT

The fixed-cockpit simulator was equipped with a typical transport flight-test instrument display (fig. 1). Special instrumentation included angle-of-attack and sideslip indicators, tail-skid ground-clearance indicator, control force readouts, data correlation counter, and individual landing gear lift-off indicators.

Two general purpose analog computers were programmed to represent the motion of the airplane in six degrees of freedom. Figure 2 shows one computer and the recording facilities. Details of the computer program are given in appendix A, equations in appendix B, and scaling limits in appendix C.

A "real world" visual scene (unity magnification) was provided by closed-circuit TV projection onto a screen 11 feet forward of the pilot. The field of view was approximately 33° vertically by 44° horizontally. The visual scene was generated by a runway model (scale 1:300) on a moving belt driven past a camera that was servo-driven in the other five degrees of freedom (fig. 3). This provided the pilot with a simulated runway 10,000 feet long by 150 feet wide.

A conventional transport wheel-type control arrangement was used. The use of spring-damper systems to represent control forces provided only an approximation to the feel of the longitudinal control due to the absence of aerodynamic force feedback in the simulator. The control column was equipped with a stall warning shaker. The rudder pedals were equipped with differential toe brakes and rudder-pedal-actuated nose-wheel steering (RPS).

Two throttles regulated the engine thrust. Equipment limitations dictated that one throttle control both left engines and another the right engines. Individual engines could be throttled or "failed" at the computer console.

Auxiliary equipment included an engine noise generator and a pneumatic pilot seat for simulating "motion." (See appendix D for details.)

TEST CONFIGURATIONS

A Douglas DC-8 airplane, with a standard-leading-edge slotted wing and powered by four JT4-A-3/5 engines, was considered representative of the current class of turbojet transports and was chosen as the subject airplane for the purpose of simulator validation. The geometry of this aircraft is shown in figure 4. Reference 7 was the source of the aerodynamic data.

Four combinations of weight and c.g. position were simulated, representing nominal extremes in weight and c.g. location: (1) heavyweight, aft c.g., (2) heavyweight, forward c.g., (3) lightweight, aft c.g., and (4) lightweight, forward c.g. These corresponded to weights of 200,000 lb and 300,000 lb, and c.g. locations of 19 percent $\bar{c}$ and 32 percent $\bar{c}$. Emphasis was placed on the heavyweight, forward c.g. configuration as the critical configuration for the take-off flight-test maneuvers. Takeoffs were performed using 15° and 25° flaps. Reference 8 details operation of the airplane.

EXPERIMENT PROCEDURE

Tests fell into two general categories. Initial tests were performed to compare the performance and dynamic characteristics of simulator and airplane. Then typical flight-test and airworthiness certification maneuvers (refs. 1 and 2) were "flown" as an overall check of the simulation capabilities for certification work. Each maneuver is described in the corresponding subsection of the Discussion and Results.

The simulator was flown by NASA, FAA, and airframe manufacturer pilots; the FAA and company pilots had participated in the original certification flight tests. All pilots were experienced in the use of research simulators. Portions of the simulator tests were observed and checked by the same FAA flight-test engineer who participated in the certification of the aircraft. The degree of simulation validity was based on qualitative pilot opinions on similarity of "feel and handling" of the simulated airplane as well as quantitative duplication of the flight-test results, as reported in references 9 and 10.

Smooth air and sea-level standard conditions were assumed for the analog computation. However, for realism, zero altimeter and zero heading instrument readings were avoided as initial conditions.

Takeoff Settings and Reference Speeds

Table I is a compilation of the flap setting, stabilizer setting, and reference speeds that correspond to the two weights and two centers of gravity flown.

TABLE I.- TAKEOFF SETTINGS AND REFERENCE SPEEDS

	200,000 lb c.g. = 19 percent $\bar{c}$	200,000 lb c.g. = 32 percent $\bar{c}$	300,000 lb c.g. = 19 percent $\bar{c}$		300,000 lb c.g. = 32 percent $\bar{c}$	
δ_F, deg	25	25	15	25	15	25
i_H, deg	3.6 ANU	2.0 AND	5.5 ANU	5.5 ANU	1.2 AND	1.2 AND
V_1, knots	118	118	142	137	142	137
V_R, knots	123	123	153	148	153	148
V_2, knots	140	140	163	158	163	158
$V_{s_{min}}$, knots[a]	106	106	132.5	128	132.5	128
Time to 100 knots, sec	19	19	30	30	30	30

[a]These are reference speeds and do not reflect the actual change in stall speed with c.g. shift.

Derivation of the recommended stabilizer settings for the subject airplane is discussed in reference 11.

DISCUSSION AND RESULTS

Initial Tests

Simulation of the complete takeoff, including the ground roll, requires computation complexity beyond that associated with the usual low-speed simulator flying qualities study. Contributing to this complexity are the reactions of the landing gear to the ground, the aerodynamic effects of ground proximity, and the large variations in speed and aircraft attitudes. Accurate duplication of the airplane's performance is a requirement, due to the interrelationship between airplane handling qualities and performance, particularly near the ground at marginally low thrust levels.

Initial trials of the simulator showed discrepancies between simulator and flight characteristics. Rotation characteristics were different and minimum lift-off speeds were 6 to 8 knots below those expected. These discrepancies were attributed to inaccuracies in the representation of ground effect on the lift and pitching moment. Adjustments were made to these values as shown in figure 5. The rotation difficulties were corrected by reducing the nose-down pitching moment due to ground effect and by compensating for the downwash variations over the tail with varied flap settings. In order to correct the lift-off speed disagreement, the beneficial lift increment due to ground effect was decreased. This adjustment was somewhat arbitrary -- it is possible that the basic lift characteristics "out of ground effect" were in error at the high angles of attack (refer to discussion of stall speeds, p. 11) and that this was compensated for by the change in ground effect lift. The simplifying assumption was used that the drag coefficient corresponding to a discrete α is unchanged by ground effect.

Additional comments regarding details of simulation techniques may be found in appendix D.

Acceleration.- Acceleration checks were conducted for 15° and 25° flap configurations and at two T/W conditions (all-engines-operative and one-engine-inoperative cases at a standard takeoff gross weight of 300,000 lb). The aircraft was in the normal taxi attitude and trimmed for takeoff.

Comparison of the simulator accelerations with the flight-test results (fig. 6) shows good correlation, with the simulator points generally falling within the flight-test scatter. Simulator aerodynamic drag began to become excessive at 0° angle of attack with the 25° flap configuration at speeds in excess of 140 knots as shown by low acceleration. This effect was ignored since rotation was initiated at 148 knots or less and drag at the angles of attack used during rotation and subsequent climb was accurate.

Ground handling.- Because the simulator was of the fixed-cockpit type, it could not provide the motion cues normally available in the real world. However, results of the runway center-line tracking task indicate that visual cues necessary to assist the pilot in accomplishing and holding center line are available in a two-dimensional scene.

The increment of directional control effectiveness gained by the use of rudder-pedal-actuated nose-wheel steering was similar to that of the actual airplane. Numerical examples of this result were obtained in the V_{MC_G} tests. The ability to produce bank angles during the ground run has been used by pilots to provide additional directional control. This effect was reproduced in the simulation.

Directional control via differential braking of the main wheels was similar to that of the actual airplane. It was found necessary to reasonably simulate the brake "feel" characteristics in terms of pedal angle and applied forces in order for the pilot to make normal use of brakes.

In the early stages of the simulation one pilot reported that he could not produce bank angles on the ground at as low speeds as in the airplane. When the maximum aileron wheel throw was reduced from $\pm 100^{\circ}$ to the more nearly correct value of $\pm 80^{\circ}$, and the scaling appropriately changed, the pilot reported the proper response from the simulator. The pilot was unaware of the changes. The proper bank angle would have resulted before the change had he used a larger wheel deflection, since the maximum lateral control power was unchanged. This wheel-gain change incident provides some evidence that pilots were applying cockpit control deflections in the simulator of the same magnitude as they did in the actual airplane, and they expected to elicit the same results. Evident throughout the simulation was the need for precise duplication of the airplane's primary cockpit controls, both in geometry and in static and dynamic-force characteristics.

Takeoff transition.- The transition of the airplane from the runway to the climb was examined by studying the loss in acceleration due to the rotation maneuver and the performance demonstrated in reaching a height 35 feet above the runway surface. Rotation times and the relationship of lift-off speed to ground angle were checked. Rotation time is the time between the rotation elevator input and main gear lift-off.

Simulator results indicate that the loss in acceleration due to rotation was approximately 6 percent in excess of that experienced in the flight-test runs. However, pilots commented that in the simulator the decrease in acceleration appeared slightly less than in actual flight.

The time required to rotate to the lift-off attitude, following the control input, is shown in figure 7 for various second segment (takeoff thrust on three engines, takeoff flaps, gear retracted) climb (T-D)/W.[1] Average rotation times ranged from 2.9 seconds at the higher (T-D)/W to 3.5 seconds at the low (T-D)/W levels. Corresponding flight-test times appear slightly longer, ranging from 3.1 to 4.1 seconds. This resulted from the pilots rotating the simulated airplane more abruptly to higher lift-off attitudes. Ground angle at lift-off is presented as a function of the ratio of lift-off speed to the 1g stall speed (fig. 8) and is displayed in this manner so the

[1]Second segment thrust and drag are measured at V_2 speed which is the speed attained at the end of the takeoff distance (when a height of 35 ft has been attained).

flight-test values may be included independent of the gross weight. Simulator points fall within the flight-test scatter.

Figure 9 shows time to 35 feet as a function of (T-D)/W. Note the increase in scatter of test points as (T-D)/W is decreased to marginal values. This demonstrates the increased dependency of the maneuver on pilot technique as T/W values become low. Simulator points and flight-test values agree well within the normal (T-D)/W range for heavyweight takeoff. During the simulator runs (T-D)/W was varied by varying thrust and leaving weight constant; in the flight tests the weight was varied. Slightly different results at the high and low (T-D)/W may be due to the different reference (stall) speeds corresponding to the various weights. At high (T-D)/W simulator time to 35 feet was short and speed was low; while at the low (T-D)/W, time was long and speed slightly high. This indicates a difference in pilot technique after lift-off. In the simulator at the higher performance levels, the pilots tended to raise the nose prematurely to stop longitudinal acceleration shortly after lift-off and to gain altitude abruptly, while in flight, the acceleration was more slowly reduced to zero after lift-off in order to attain V_2 at 35 feet. This tendency as well as the previously mentioned tendency to overrotate before lift-off may be attributable to the absence of a dangerous or hazardous element in the simulator as compared to the flight-test situation. Also influencing this tendency could be the lack of motion cues which serve to assist the pilot in damping the pitching motion.

Climb gradients.- The lift and drag relationships of the simulator were verified by documenting the gradients in the various climb segments at 300,000 lb gross weight (out of ground effect) and comparing them to the flight-test results.

Results of the first segment climb gradient (takeoff thrust, takeoff flaps, gear extended) are plotted against airspeed for 15° and 25° flap configurations in figure 10. Curves are presented showing three-engine and four-engine performance. Figure 11 shows first, second, and final segment climb gradients versus engine thrust level at the speeds noted with three engines operative.

For all takeoff climb gradients, simulator check points fell within the flight-test scatter in the takeoff test speed range. As the stall speed was approached, the performance on the simulator proved to be greater than the flight-test values by as much as 1 percent excess climb gradient. This may have been due to the use of incorrect lift and drag data near the stall where extrapolation of the flight data was required; a second source of error was the programming simplifications discussed in the section on stall speeds. These approximations resulted in a higher L/D than that of the airplane within the 10-knot speed region above the stall. These effects would provide erroneous gradients only for the heavyweight three-engine or extremely low T/W four-engine condition within this speed range. These conditions were not encountered in the tests.

Stall speeds.- The 1g stall speeds (the speed at which the lift is no longer equal to the weight component perpendicular to the flight path) were

determined out of ground effect at idle thrust and are compared with the flight-test values in the following table.

TABLE II.- "ONE-G" STALL SPEEDS

Flap setting, deg	Gross wt = 300,000 lb; c.g. = 19 percent $\bar{c}$	
	$V_{s_{1g}}$, simulator, knots	$V_{s_{1g}}$, flight test, knots
25	132.5	133.5
15	139	139.5
0	151	165.5

For ease of simulation, C_L versus α was programmed as a basic curve for the 0° flap condition, and C_L was biased linearly for the various flap deflections (as shown in the sketch below). This resulted in the angle of attack at stall being independent of flap setting; in reality the airplane stalls at a lower angle of attack in the zero flap configuration. Accurate representation was provided for the 15° and 25° flap cases, with the result that stall speed was incorrect at zero flap setting. Additionally, the exact shape of the lift curve near the stall was not readily available and was therefore estimated as indicated. A stall situation in the simulator was not accompanied by a roll-off or a pitch-down because the addition of this complexity was not warranted by the present test objectives.

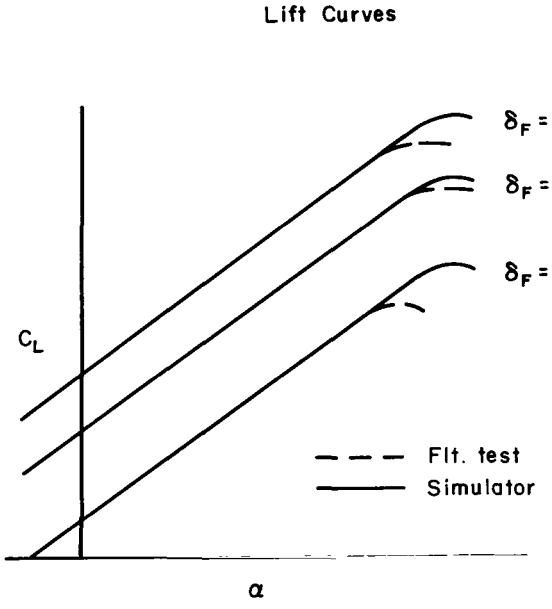

Lateral-directional characteristics.- Dynamic response checks of the simulator were conducted by exciting the Dutch roll with a rudder kick and recording the subsequent oscillation. All simulator flights were without yaw damper. In figures 12-14 these results are shown with those obtained from flight test (ref. 12). The flight-test points should not be directly compared to simulator points, as the flight-test points correspond to lighter gross weights and a higher altitude (9000 ft).

Figure 12 presents the Dutch roll periods with good agreement and demonstrates a normal decreasing trend with increasing airspeed.

The general level of damping was quite low, requiring 10-26 seconds to damp to one-half amplitude as shown in figure 13. With this low damping the discrepancy between flight and simulator was not readily apparent to the pilots; therefore, determination of the cause for disagreement was not considered worthy of a large expenditure of analysis time. Some discrepancy can be attributed to the erroneous use of approximately 40-percent excessive yaw damping C_{n_r} on the simulator.

The ratio of roll angle to equivalent side velocity $|\varphi|/|V_e|$ of the simulator was less than that demonstrated in flight tests, being of the order of 0.30° to 0.36°/ft/sec as compared to flight-test values of 0.43° to 0.53°/ft/sec (fig. 14). Hand calculations to check $|\varphi|/|V_e|$ yielded values from 0.30° to 0.39°/ft/sec, verifying that the simulator was properly representing the programmed derivatives.

The evaluating pilots agreed that the Dutch roll characteristics were representative of the DC-8 with the exception that immediately after lift-off at speeds below the normal lift-off speeds a lateral-directional oscillation was frequently excited which was not evident during flight testing of the airplane. It was not established whether this was due to other lateral-directional factors not accurately simulated or whether lack of motion cues tended to produce more pilot induced oscillation in the simulator than occurred in actual flight. In general, however, the pilots felt that this discrepancy did not seriously interfere with their ability to conduct evaluations.

Continuous takeoff.- As the primary purpose of the simulator is to investigate abnormal situations, relatively few normal continuous takeoffs were performed specifically for data. However, pilots reported that, as a whole, the simulation was a good representation of a subsonic jet transport takeoff. Figure 15 shows a representative simulator takeoff time history.

Certification Tests

The initial tests discussed in the preceding sections were essentially a check on the performance of the simulator. Results indicated a satisfactory match of airplane characteristics. Therefore, additional tests were conducted using as piloting tasks several of the maneuvers associated with current airworthiness certification. Interest in these later tests centered around pilot-airplane performance, recognition and reaction times, and pilot subjective assessment as to the fidelity of simulation.

Accelerate-stop tests.- The accelerate-stop (rejected takeoff, RTO) test provides the information required to determine the runway distances and times required to stop should the pilot refuse or reject the takeoff for reasons of engine failure or other abnormality. Of major interest (in a research sense) are the relative contributions of basic airplane drag, spoilers, brakes, reverse thrust, etc., to deceleration (refs. 13 and 14), as well as the controllability during the stop.

The simulator was not equipped with the handwheel which is normally at the pilot's left hand for nose-wheel steering while taxiing and at low speeds, so the pilot had to make all directional corrections with the rudder pedals, making it difficult for him to maintain full braking with the toe pedals.

Engine failure recognition times varied from 1 to 3 seconds, while failure of an outboard engine in the airplane was usually identified in less than 1 second. Evident throughout the runs were the excessive distances required to stop as a result of this extra delay in recognition and/or reaction by the pilot. Contributing to this is the fact that acceleration

continues for an instant after the throttles have been abruptly retarded due to the engine time constant which permits only a slow thrust decay. Pilot recognition of an engine failure must be obtained from the visual scene in the simulator because of the lack of lateral motion cues. During V_{MC_G} tests, poor visual system response was detected; see discussion on minimum ground control speed.

To check the actual stopping performance, nonpiloted runs were made; the average recognition and reaction times (for power reduction, spoiler deployment, and wheel braking) used were obtained from flight tests (ref. 9). The simulator data of time and distance to stop then fell within the DC-8 flight-test scatter (fig. 16). The nonpiloted runs were made using $\mu = 0.136$ and $\mu = 0.08$ to represent typical stops on wet runways and ice, respectively. Braking coefficients of friction vary with speed and are generally higher at low speeds (see appendix A). For simplicity μ was assumed constant at 0.28 for dry runways.

While reverse thrust was available on the simulator, no performance comparison was made. For simulation of advanced transport aircraft that may use reverse thrust, this should be included even though such effects as reingestion from adjacent engines and induced flow changes affecting the wing lift (and thus the normal force available for braking) are difficult to estimate.

It appears that including a high response visual system and lateral motion capability would permit satisfactory simulation of rejected takeoffs.

Three-engine takeoff.- A large portion of the certification performance requirements must be met with one engine made inoperative at some point during the takeoff; hence it was desirable to match the airplane characteristics under these conditions.

As in normal operation, takeoffs were continued after engine failure at speeds above V_1. Of primary interest was lateral-directional controllability and flight-path control. Some engine failures were scheduled while others were "surprise cuts." Following the failure the rudder (along with the RPS on some runs) was used as the primary control in counteracting the resultant yawing moments, and lateral control was used as necessary to hold the wings level. Thrust was left at the takeoff value on the remaining three engines. The initial climb was then conducted at V_2 instead of the V_2 + 10 knots speed used for the four-engine takeoff.

The majority of these tests involved failure of an outboard engine; however, an occasional surprise cut of an inboard engine was made to evaluate the recognition times. Recognition times for the inboard failures were quite varied but were approximately 1 second longer than required for recognition of an outboard failure (as discussed in the section on accelerate-stop tests).

The pilots were able to maintain control and continue the takeoff without difficulty from engine failures occurring at speeds ranging upward from V_1. Pilots reported that the response of the simulator to an engine failure was much like that of the airplane, but slightly milder, perhaps due to the combination of poor visual system response and the lack of motion. Also, a

lateral-directional oscillation was frequently excited which was not evident in the airplane and added to the pilot's task in controlling the three-engine climbout (see section on lateral-directional characteristics).

Takeoff with incorrect trim.- Prior to a number of the takeoffs the horizontal stabilizer trim was purposely set to an abnormal value -- in some cases without the pilot's knowledge. The result of incorrect stabilizer trim (mistrim) is not obvious to the pilot until V_R is reached, when it is revealed by the unusual forces required to rotate.

Full airplane nose down (AND) trim, forward c.g., and maximum takeoff gross weight are an extreme combination that requires more pitching moment for rotation than is available at the normal V_R speed. If the airplane should inadvertently be trimmed to this condition, whether by oversight, error, or mechanical or electrical failure, the pilot would not, upon applying the normal elevator input, obtain enough pitching moment to rotate the aircraft. Since V_1 speed has been exceeded, there is no choice but to continue the takeoff. The desired pilot response in this particular case is for the pilot to hold full back on the control column and start to retrim. When sufficient speed has been attained the aircraft will rotate and lift off, though somewhat farther down the runway than in a normal takeoff. Such incidents have occurred in actual flight. If the pilot is not forewarned, he might, most naturally, assume a control malfunction and resort to increasing back pressure as well as releasing, and reapplying force. Thus, if the mistrim condition is not detected and corrected during the initial portion of the takeoff run, the airplane can go off the end of the runway before lift-off occurs.

In order to compare pilot reaction between simulator and flight, the aforementioned situation was presented to several pilots in the simulator without their prior knowledge. One reduced thrust to idle and attempted a stop (at a speed in excess of V_1), going off the end of the runway; one assumed a simulator malfunction and called for reset of the computer; another, who knew the consequences of extreme airplane-nose-down trim, held the column full back until lift-off and retrimmed. Both the first and last responses have occurred in flight.

In the simulator pilots were able to identify accurately the amount and direction of incorrect trim from the control input required to rotate and the resulting rotation pitch rate. This indicated that the simulator and the airplane provided the same subjective impressions of the mistrim condition. It was felt that the simulator was adequate for investigating trim effects on takeoff characteristics.

Unstick speed.- The unstick speed is the speed at which the main gear lifts off the runway during takeoff. Of major interest is the minimum possible value, V_{MU}, that can be obtained without taking advantage of the dynamic effects associated with abrupt elevator inputs and yet yields acceptable handling characteristics.

Simulator V_{MU} results were within 3 knots of flight tests. Figure 17 is a typical time history comparison. The pilots tended to climb more

abruptly in the simulator than in the flight test, sacrificing acceleration for climb angle immediately following lift-off, as discussed in the section on takeoff transition. Aside from this difference in piloting technique several slight differences between the airplane and simulator in figure 17 are:

1. The airplane had a lower pitch response because it was slightly heavier, had a slightly lower thrust-to-weight ratio, and carried less ANU trim.

2. The airplane required greater stick forces during the rotation input; the simulator curve in figure 17 is derived from the stick position recording and does not include the transient force contributions due to control damping and inertia. The airplane stick force trace was read out directly from a force transducer.

3. The simulator stick force trace had less high frequency content due to different piloting technique and/or the lack of cockpit motion feedback, as well as to the difference in obtaining the force readout as mentioned in 2.

At progressively lower T/W the acceleration to V_2 after lift-off in the simulator becomes increasingly dependent on pilot technique in airspeed control and upon basic handling qualities. The same was true of the aircraft.

A rapid elevator input at certain speeds can speed rotation and induce lift-off below V_{MU} due to dynamic effects associated with the high pitching rate. This effect was demonstrated in the simulator and is discussed in appendix E.

The hazardous V_{MU} maneuver can be studied successfully on the simulator. The addition of such environmental effects as the stick shaker and stall buffet (by means of pneumatic seat cushion or other limited vertical motion) add significantly to the realism of this maneuver.

Ground minimum control speed.- Records were taken of the unavoidable excursions from runway center line experienced in the simulator as a result of outboard engine failures. The pilot would be given a "surprise" engine cut and would, upon recognition of which engine had failed, react with rudder (in some cases full rudder) to oppose the yawing moment caused by the engine failure. The minimum speed at which, following an outboard engine failure, the maximum lateral deviation from the center line can still be held to 15 feet was termed V_{MC_G}. Reference 15 provides an example of the procedures involved in minimum control speed testing.

Initial simulator runs yielded data quite different from data of the flight tests. Lateral deviations could be arrested at lower speeds in the simulator than in the airplane. Reprogramming the rudder control to represent more accurately the rudder power and the rudder servo-system lag moved the curve to speeds above the flight-test values as shown in figure 18. Additionally, the slope of the lateral deviation versus the V_{EF} curve was much too shallow; for example, in the actual airplane an engine cut 10 knots below V_{MC_G} required that the pilot reduce thrust on the opposing engines to keep the

aircraft within the confines of the runway. In the simulator an outboard engine failure 10 knots below the determined V_{MC_G} value could be controlled within the runway boundaries with rudder alone. As in the case of the rejected takeoff, the pilot must have good engine failure cues to successfully accomplish this maneuver. Part of the difficulty in the simulator was traced to the deadband and sluggish response of the lateral and heading drives for the visual system camera which delayed by a fraction of a second the possibility of the pilot's recognition of the engine failure. Also contributing to this may have been the absence of the lateral motion cue.

A special technique (used only in the simulator as a substitute for motion cues), which consisted of giving the pilot a verbal cue of the word "cut" at engine cut (the pilot having prior knowledge of the engine to be cut but not the intended cut speed), produced a y_p versus V_{EF} curve with the same slope and displaced only a few knots below the flight-test data. The verbal cue eliminated the engine-failure recognition time and the decision time but not the pilot reaction time.

While not able to use the simulator to determine engine failure recognition times its usefulness for parametric studies of ground control characteristics was demonstrated.

Air minimum control speed.- The in-flight minimum control speed was determined by slowing the airplane until full rudder control was required to maintain a steady heading with an outboard engine inoperative. During flight tests of this nature, it is common practice for the wind screen to be overlayed with a transparent sheet of plastic on which are clearly scribed various angles with reference to the horizontal. Thus, the pilot has a very sensitive roll attitude indicator with which he alines the horizon. The overlay was not used for this series of simulator tests, since the visual scene was not sufficiently accurate, leaving the attitude gyro as the primary roll reference. The indicator, although quite small, gave acceptable (for simulator use) bank angle information.

As V_{MC_A} is below the heavyweight stall speed, this test was conducted at the 200,000 lb gross weight and at aft c.g. Results were obtained for wings level and for a 5° bank angle assisting the rudder (bank away from the inoperative engine).

With an asymmetric thrust of 14,600 lb and with 5° of bank the simulator V_{MC_A} was determined to be 111 knots, 5 percent below the flight-test value (fig. 19). That the simulator produced approximately 11-percent excess rudder power ($C_{n_{\delta_r}}\delta_{r_{max}}$) was later substantiated by the V_{MC_G} results. It was discovered that the rudder pedal stops were not supported rigidly enough and may have contributed to this error by permitting excess rudder travel.

One of the pilots noted, in a large number of tests on transport airplanes (including the reference airplane), that for each degree of bank away from the dead engine, an approximate 4-knot reduction in minimum control speed can be realized. The simulator displayed this same sensitivity to bank

angle. Wings-level V_{MC_A} was approximately 129 knots, or 18 knots above the 5^o bank value, providing a $dV_{MC}/d\varphi$ = -3.6 knots/deg.

As indicated by figure 19, approximately 60 percent of available wheel throw away from the dead engine was required in order to hold 5^o bank angle and a constant heading. About 12 percent of available wheel throw was used at the wings level minimum control speed.

It was concluded that the V_{MC_A} task was realistically and accurately represented. The simulator is especially well-suited to parametric studies in hazardous flight ranges. For example, the effect of weight on V_{MC_A} and the accompanying handling characteristics can be safely investigated.

CONCLUDING REMARKS

A piloted fixed-base takeoff simulation was developed for study of advanced transport aircraft airworthiness requirements and handling qualities. Confidence in the simulation was realized by successful duplication of the takeoff certification tests of a subsonic jet transport. The following remarks can be made regarding this simulator validation phase.

Since many of the takeoff certification maneuvers are conducted near the ground where airplane performance, handling qualities, and piloting techniques are intimately related, accurate representation of performance (as well as dynamic response) is essential.

As ground effect exerts a significant influence on the rotation and lift-off characteristics, accurate data are essential. Available information on ground effect appears inadequate, suggesting a requirement for additional research effort.

The pilots felt that the continuous takeoff on the simulator was realistic, but the lack of motion was evident and decreased the realism in takeoffs involving engine failures. Motion appears desirable for investigations involving dynamic asymmetric thrust conditions (e.g., minimum control speed tests and refused takeoffs), where prompt engine failure recognition is an important factor and for tests where lateral-directional and longitudinal oscillatory motions would modify pilot control input.

While the simulator proved not to be useful for determining engine failure recognition times, its usefulness was demonstrated for parametric studies of ground control characteristics.

Pilots treat the simulated airplane in a less conservative manner than the actual airplane -- rotating more abruptly and holding higher pitch attitudes during the initial climb. This may be attributable to the absence of the "anxiety factor" and possibly to the lack of motion cues.

The added environmental realism obtained from the pneumatic seat cushion, used both to simulate passing over the runway tar strips during takeoff roll and for prestall buffet, aided in establishing the proper psychological involvement on the part of the pilot.

In general, the degree of visual scene image quality required for takeoff is not so great as that required for studies involving landing approach and flare. However, there is the desirability of providing peripheral visual cues -- near-visual-field information for V_{MU} tests, far-field cues (horizon) for V_{MC_A} studies, and both for continuous takeoffs. While the visual scene response was adequate for many of the maneuvers performed, a high level of dynamic response of the camera drive in the lateral and yaw modes is required for maneuvers involving engine failure.

The simulator is especially well suited to parametric studies in hazardous flight ranges. For example, the effect of weight on V_{MC_A} and the accompanying handling characteristics can safely be investigated.

The simulation has shown its potential usefulness as a tool in flight test guidance and training of the initial crews.

Ames Research Center
National Aeronautics and Space Administration
Moffett Field, Calif., Jan. 17, 1966

APPENDIX A

COMPUTER PROGRAM PARTICULARS

AXES SYSTEM

The computer was programmed to represent the airplane in six degrees of freedom. The equations are presented in appendix B. For simplification and accessibility to the variables to be recorded, the force equations were derived with reference to wind axes while the moment equations were written about the body axes (ref. 16). The forces and moments result from a combination of aerodynamic effects and gear reactions due to contact with the ground. The airplane was considered a rigid body and moments were taken about the center of gravity. It was found helpful to reference airplane physical dimensions to some fixed point near the c.g. -- in this program, the aerodynamic center was used. Thus, the distance from the reference point to the c.g. is the only change in dimension required when c.g. location is changed.

Small-angle approximations were used with regard to α, β, γ, and θ. Thus, $\cos \alpha = 1$ and $\sin \alpha = \alpha$, etc.

ALTITUDE SCALE CHANGE

A scale change was necessary to provide adequate resolution in altitude during operation near the ground as well as an operating range of several thousand feet. This provided 1 volt/ft for those circuits requiring sensitive altitude signals, for example, landing gear reactions and ground effect. When the altitude exceeded 90 feet, the scaling changed to 0.025 volt/ft in order to allow operation of the program at altitudes as high as 4000 feet above the ground level. The choice of 90 feet as a reference point was quite arbitrary, but was selected as high enough to be above the altitude where ground effect was significant.

FORM OF AERODYNAMIC DERIVATIVES

Aerodynamic forces and moments were generated from conventional derivatives (ref. 7) represented as constants or linear functions of angle of attack. The moment derivatives were converted from stability axes to body axes before being programmed into the computer. It may, in some cases, be expeditious to perform this conversion in the computer at the cost of additional computation equipment.

LATERAL-DIRECTIONAL CHARACTERISTICS

Evaluation of the handling qualities, especially under abnormal conditions (e.g., asymmetric thrust, etc.), requires a reasonable representation of the lateral-directional characteristics of the simulated airplane. The values

of a number of the stability derivatives are dependent on lift coefficient C_L. This adds complication to the simulation problem because of the large variations of angle of attack and flap configuration encountered in the takeoff maneuver. Because the number of computer components available is limited, approximations were necessary in programming some of the derivatives. Most of the stability derivatives were provided as constants while three (C_{l_β}, C_{l_r}, and C_{n_p}) were represented as linear functions of angle of attack; C_{Y_p} and C_{Y_r} were set equal to zero. A higher degree of accuracy would have been realized if it had been practical to represent: (1) C_{n_p}, C_{l_r}, C_{l_β}, and C_{Y_p} as functions of C_L; and (2) C_{n_β}, $C_{n_{\delta_a}}$, and $C_{l_{\delta_r}}$ as functions of α. Close scrutiny of the variation of each derivative within the desired testing range is essential for accurate representation of each different airplane simulated.

LANDING GEAR REPRESENTATION

Various methods of representing landing gear forces and an extensive bibliography on landing gear dynamics are presented in reference 17. A linear spring-damper system represented the nose gear in the present study. The main gear shock struts were individually represented by a nonlinear spring and linear damper. The circuit for computing landing gear forces is shown in figure 20. It is recognized that strut damping characteristics are not actually linear, but the assumed linear action served satisfactorily in the absence of more detailed information.

As the tires serve to absorb most of the sharp, abrupt loading, it was considered worthwhile to represent them in the main gear equations for later tests involving landing as well as takeoff. This detail is desirable for landing studies, but the need is less apparent for studies involving only takeoffs from smooth runways.

TIRE ROLLING, BRAKING, AND SIDE-FORCE COEFFICIENTS

Values of the rolling resistance coefficient, μ_r, of 0.020 were suggested in references 13 and 18, and of 0.017 in reference 9. The higher value resulted in acceleration slightly less than that measured in the flight tests. A value of 0.016, which gave good agreement with flight data, was selected.

A simplified approach was taken in the generation of the landing gear tire braking and side (cornering) force coefficients. These coefficients are functions of runway surface, speed, tire pressure, tire temperature, tire size, tire tread, etc., as evidenced in references 19 to 25.

As mentioned in the discussion of the accelerate-stop tests, an average effective value of 0.28 was used for the dry runway braking coefficient where the braking force was equal to the product of the coefficient and the vertical load on the tire (F_g), or

$$\text{braking force} = \mu_b F_g$$

Maximum μ_b is obtained by the pilot fully depressing the toe brakes and holding them in this position, simulating an automatic braking system. The airplane actually had a thumper modulated antiskid system to guide the pilot's braking pressure. Since most advanced aircraft to be researched will have automatically modulated brake systems to provide near maximum braking efficiency, no attempt was made to install and simulate thumpers in the simulator.

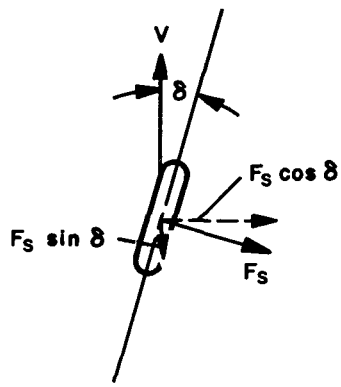

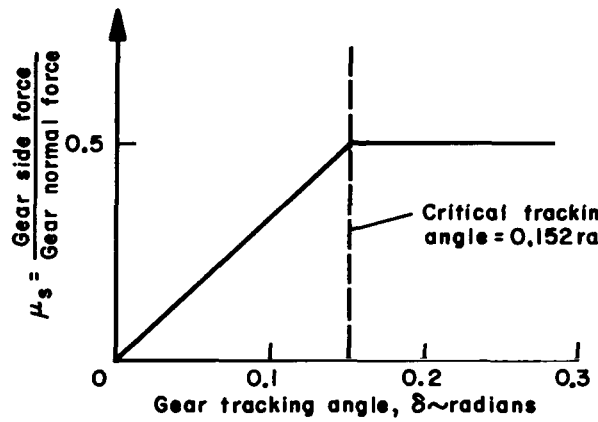

The sketch above illustrates the method of generating cornering forces. Shown is a top view of a wheel with its plane of rotation at an angle, δ, with the direction of motion. Due to the tracking angle δ, there is generated a cornering force F_S parallel to the axle which can be resolved into components $F_S \cos \delta$, a side force perpendicular to the direction of motion, and $F_S \sin \delta$, a drag force opposing the forward motion. The side force, $F_S \cos \delta$, is represented in the simulator equations by

$$\text{side force} = F_S \cos \delta \doteq F_S = F_g \frac{\partial \mu_s}{\partial \delta} \delta$$

The simplifying assumption that $\cos \delta$ equals unity restricts the use of the equations to programs where the steering angle will always be reasonably small (e.g., $\delta < 0.25$ radian). The simulator maximum μ_s of 0.5 is reached when the critical tracking angle of 0.152 radian (8.7°) is exceeded. This critical tracking angle actually depends on tire, runway surface, and speed, and can be as high as 0.35 radian (20°) as shown in reference 20. The decelerating component $F_S \sin \delta$ was not included in the simulation.

TAIL STRIKE CIRCUIT

In order to simulate the pitch attitude restriction imposed by the tail contacting the runway surface, a nose-down pitching moment was provided through a high-gain feedback when the tail clearance reached zero. This was the analog equivalent to placing a strong spring under the tail. The gain or spring constant was determined by experimenting with several values and choosing one which did not excite an unstable oscillation. This simplified representation provided only the pitching moment but not the vertical and longitudinal forces that would normally accompany a tail strike.

CONTROL SYSTEMS AND ENGINE RESPONSE

First-order systems, output = input $(1 - \epsilon^{-t/\tau})$, were used to represent engine and rudder responses during dynamic minimum control speed tests. Time constants τ of 1.8 and 0.5 sec were assumed for the engines and rudder system, respectively. All other control systems were simulated with instantaneous response.

In addition, the thrust lapse with increasing speed was accounted for by a linear approximation. In order to avoid a decelerating force resulting from the thrust lapse term when engines were reduced to idle, the term KV (appendix B) was switched to zero when thrust was reduced below a value 50 percent greater than idle.

DATA ACQUISITION

In addition to the 16 channels of analog recording capability, simple track-and-store circuits (each comprised of an integrator wired as a voltage follower plus an electronic comparator relay to switch off the input at the appropriate time) were utilized to provide a precise direct readout of the speed at lift-off of nose and main wheels without need for interrupting the takeoffs.

COMPUTER COMPONENT REQUIREMENTS

Computation equipment requirements for the program described in this document were as follows (in approximate quantities):

Integrating amplifiers	20
Summing and inverting amplifiers	110
Potentiometers	175
Servo-multipliers (5 cups each)	5
Electronic multipliers	12
Comparators (relays)	12
Function generators	4
Resolvers	2

APPENDIX B

EQUATIONS OF MOTION

Roll:

$$\dot{p} = \frac{\rho V^2 Sb}{2I_X}\left[C_{l_\beta}\beta + C_{l_{\delta a}}\delta a + C_{l_{\delta r}}\delta r + (\Delta C_l)_{spoilers}\right] + \frac{\rho VSb^2}{4I_X}\left(C_{l_p}p + C_{l_r}r\right)$$

$$+ \frac{i_T}{I_X}\left[y_1(T_1 - T_4) + y_2(T_2 - T_3)\right] + \frac{y_{mg}}{I_X}(F_L - F_R) - \frac{h_o}{I_X}\mu_{s_{\delta_{mg}}}\delta_{mg}(F_L + F_R)$$

Pitch:

$$\dot{q} = \frac{\rho V^2 S\bar{c}}{2I_Y}\left[C_{m_o} + C_{m_\alpha}\alpha + C_{m_{\delta e}}\delta e + C_{m_{i_H}}i_H + C_{m_{\delta_F}}\delta_F + (\Delta C_m)_{LG} + (\Delta C_m)_{spoilers}\right.$$

$$\left. + (\Delta C_m)_{GE} + (\Delta C_m)_{tail\ strike}\right] + \left(\frac{I_Z - I_X}{I_Y}\right)rp + \frac{\rho VS\bar{c}^2}{4I_Y}\left(C_{m_q}q + C_{m_{\dot{\alpha}}}\dot{\alpha}\right)$$

$$+ \frac{d}{I_Y}T + \frac{l_{ng} - l_{cg}}{I_Y}F_{ng} - \frac{l_{mg} + l_{cg} - h_o\theta}{I_Y}(F_L + F_R)$$

$$- \frac{h_o}{I_Y}(\mu_L F_L + \mu_R F_R)$$

Yaw:

$$\dot{r} = \frac{\rho V^2 Sb}{2I_Z}\left[C_{n_\beta}\beta + C_{n_{\delta r}}\delta r + C_{n_{\delta a}}\delta a + (\Delta C_n)_{spoilers}\right] + \frac{\rho VSb^2}{4I_Z}(C_{n_r}r + C_{n_p}p)$$

$$+\left(\frac{I_X - I_Y}{I_Z}\right)pq + \frac{y_2}{I_Z}(T_2 - T_3) + \frac{y_1}{I_Z}(T_1 - T_4) + \frac{y_{mg}}{I_Z}(\mu_R F_R - \mu_L F_L)$$

$$+ \frac{l_{ng} - l_{cg}}{I_Z}\mu_{s_{\delta_{ng}}}\delta_{ng}F_{ng} - \frac{l_{mg} + l_{cg}}{I_Z}\mu_{s_{\delta_{mg}}}\delta_{mg}(F_L + F_R)$$

Longitudinal acceleration:

$$a_x = \dot{V} = \frac{T}{m} - \frac{\rho V^2 S}{2m}\left[C_D(\alpha) + (\Delta C_D)_{\delta_F} + (\Delta C_D)_{spoilers} + (\Delta C_D)_{LG} + (\Delta C_D)_{GE}\right]$$

$$- g\gamma - \frac{1}{m}\mu_L F_L - \frac{1}{m}\mu_R F_R$$

Side acceleration:

$$a_y = g \sin \varphi + \frac{\rho V^2 S}{2m} \left(C_{Y_\beta}\beta + C_{Y_{\delta_r}}\delta_r\right) - \frac{1}{m} T\beta + \frac{1}{m} \mu_{s_{\delta_{ng}}} \delta_{ng} F_{ng} + \frac{1}{m} \mu_{s_{\delta_{mg}}} \delta_{mg} (F_L + F_R)$$

Vertical acceleration:

$$a_z = g \cos \varphi - \frac{1}{m} T(\alpha + i_T) - \frac{\rho V^2 S}{2m} \Big[C_L(\alpha) + C_{L_{\delta_e}}\delta e + C_{L_{i_H}} i_H + C_{L_{\delta_F}}\delta_F$$

$$+ (\Delta C_L)_{spoilers} + (\Delta C_L)_{GE} \Big] - \frac{\rho V S \bar{c}}{4m} C_{L_q} q - \frac{1}{m} (F_{ng} + F_L + F_R)$$

Euler angles:

$$\dot{\gamma} = - \frac{a_y}{V} \sin \varphi - \frac{a_z}{V} \cos \varphi , \qquad V > 0$$

$$\dot{\varphi} = p + r\alpha - \frac{a_z}{V} \beta + \dot{\psi}_w \gamma , \qquad V > 0$$

$$\dot{\psi}_w = \frac{a_y}{V} \cos \varphi - \frac{a_z}{V} \sin \varphi , \qquad V > 0$$

Angle of attack:

$$\dot{\alpha} = \frac{a_z}{V} + q - p\beta , \qquad V > 0$$

Angle of sideslip:

$$\dot{\beta} = \frac{a_y}{V} - r + p\alpha , \qquad V > 0$$

Heading:

$$\psi_i = \psi_w - \beta + \alpha\varphi$$

Pitch attitude:

$$\theta = \gamma + \alpha + \beta\varphi$$

Translations:

$$\dot{s} = V$$

$$\dot{y}_p = V \sin \psi_w + l_p r + l_p q \varphi$$

$$\dot{h} = V\gamma$$

$$h_p = h + l_p \theta + h_{o_p}$$

Rudder deflection:

$$\dot{\delta}_r = \frac{1}{\tau_r} \left(\delta_{r_{command}} - \delta_r\right)$$

Tail clearance:

$$h_{tc} = h - l_t\theta + h_{o_t}$$

Thrust (each engine):

$$\dot{T}_n = \frac{1}{\tau_e}\left(T_{n_{static}} - KV - T_n\right), \qquad \begin{array}{l} n=\text{engines 1, 2, 3, and 4} \\ KV=0 \text{ when } T_n < 1.5\, T_{idle} \end{array}$$

Landing gear reactions:

$$\dot{Z}_{ng} = -\dot{h} - (l_{ng} - l_{cg})q$$

$$Z_{ng} = -h - (l_{ng} - l_{cg})\theta$$

$$F_{ng} = k_{ng}Z_{ng} + b_{ng}\dot{Z}_{ng}, \qquad F_{ng} \geq 0$$
$$b_{ng}\dot{Z}_{ng}=0 \text{ when } Z_{ng} \leq 0$$

$$\dot{Z}_L = -\dot{h} - y_{mg}p + (l_{mg} + l_{cg})q$$

$$Z_L = -h - y_{mg}\varphi + (l_{mg} + l_{cg})\theta$$

$$F_L = f(Z_L) + b_{mg}\dot{Z}_L, \qquad F_L \geq 0$$
$$b_{mg}\dot{Z}_L=0 \text{ when } Z_L \leq 0$$

$$\dot{Z}_R = -\dot{h} + y_{mg}p + (l_{mg} + l_{cg})q$$

$$Z_R = -h + y_{mg}\varphi + (l_{mg} + l_{cg})\theta$$

$$F_R = f(Z_R) + b_{mg}\dot{Z}_R, \qquad F_R \geq 0$$
$$b_{mg}\dot{Z}_R=0 \text{ when } Z_R \leq 0$$

Gear tracking angles (restricted to zero crosswind case):

$$\delta_{ng} = \delta_{ngs} - \beta - (l_{ng} - l_{cg})\frac{r}{V}, \qquad |\delta_{ng}| \leq 0.152 \text{ radian}$$

$$\delta_{mg} = (l_{mg} + l_{cg})\frac{r}{V} - \beta, \qquad |\delta_{mg}| \leq 0.152 \text{ radian}$$
$$V > 0$$

APPENDIX C

PROBLEM SCALING LIMITS

$\dot{p}$, ... ±0.5 radian/sec^2	$\dot{\beta}$, ... ±0.33 radian/sec
p, ... ±0.5 radian/sec	β, ... ±0.33 radian
$\dot{q}$, ... ±0.5 radian/sec^2	θ, ... ±0.5 radian
q, ... ±0.5 radian/sec	s, ... ±50,000 ft
$\dot{r}$, ... ±0.5 radian/sec^2	y_p, ... ±2500 ft
r, ... ±0.5 radian/sec	$\dot{h}$, ... ±100 ft/sec
a_x, ... ±50 ft/sec^2	h, ... ±100 ft, ±4000 ft
V, ... +400 ft/sec	h_p, ... ±4000 ft
a_y, ... ±200 ft/sec^2	F_L,F_R, ... +400,000 lb
a_z, ... ±100 ft/sec^2	F_{ng}, ... +50,000 lb
$\dot{Z}_{ng}$,$\dot{Z}_L$,$\dot{Z}_R$, ... ±10 ft/sec	δ_{ng}, ... ±0.5 radian
Z_{ng},Z_L,Z_R, ... ±10 ft	δ_{mg}, ... ±0.2 radian
$\dot{\gamma}$, ... ±0.5 radian/sec	T, ... ±200,000 lb
γ, ... ±0.5 radian	i_H, ... ±0.5 radian
$\dot{\varphi}$, ... ±1.0 radian/sec	δ_e, ... ±0.5 radian
φ, ... ±0.5 radian	δ_a, ... ±0.5 radian
$\dot{\psi}$, ... ±1.0 radian/sec	δ_r, ... ±0.5 radian
ψ, ... ±1.0 radian	δ_F, ... +1.0 radian
$\dot{\alpha}$, ... ±0.5 radian/sec	μ_L,μ_R, ... +1.00
α, ... ±0.5 radian	

APPENDIX D

SIMULATION NOTES

COCKPIT MOTION REQUIREMENTS

There is reasonable evidence that pilot opinions and ratings on handling qualities obtained in fixed-base simulators are, for some maneuvers, conservative; the airplane can be expected to handle more satisfactorily than the simulator. This is attributed by some to the fact that lead terms which are normally provided by the pilot in response to motion cues must be generated by the pilot on the basis of observed instrument indications and visual scene observations, coupled with his experience. In cases where pilot induced and/or reinforced oscillations due to accelerations at the cockpit would severely degrade handling qualities in actual flight, fixed-base simulator results may be invalid.

The impression is not meant to be given that large amounts of cockpit motion are required for takeoff airworthiness studies. A fixed-cockpit simulator will suffice for most work. Lateral or side motion would permit realistic engine failure cues and, if combined with cab roll motion and washout circuitry, could possibly provide lateral-directional oscillation realism. Next, in order of value to takeoff simulation, would be vertical cab motion and cab pitch motion. However, the actual motions the pilot feels during the takeoff are the low amplitude oscillations and jolts, of the order of 1-6 cps (particularly in the lateral and vertical directions), due to aircraft structural modes driven by runway roughness inputs during takeoff roll, stall buffet during lift-off at V_{MU}, and by rough air and geometry changes (gear retractions, etc.) during climb, and, of course, by the initial responses to pilot applied control inputs. These, in all likelihood, could be provided adequately with very limited displacements that reproduce only the initial acceleration cues.

Discussions of cockpit motion may be found in references 3, 4, 5, 26, 27, 28, 29, and 30.

PNEUMATIC "MOTION" SEAT

During the takeoff roll in a fixed-cockpit simulator there is, quite naturally, no feeling of the building-up of speed as would be experienced in the airplane. This is due to the absence of any motion and the lack of outside world near-visual and peripheral fields of view. However, some substitution was provided by the pilot's pneumatic seat cushion being pulsed to simulate the aircraft rolling over the 25-foot-spaced tar runway divider strips.

During operation in the near-stall region a stall-buffet pulsation was put into the seat cushion. This along with a stick shaker (triggered by angle of attack) to warn the pilot of impending stall contributed significantly to the realism during some of the more critical maneuvers, such as determination of the air minimum control speeds and minimum unstick speed.

Reference 5 describes the use of pneumatic seat techniques by another experimenter.

OUTSIDE WORLD VISUAL SYSTEM

Visual systems designed for operational flight trainers generally do not possess the degrees of accuracy, response, and smoothness required for simulation of takeoff certification maneuvers.

The importance of a high degree of fidelity in the TV camera lateral and heading drive system became apparent early in the simulation. Sluggish response and deadband caused the pilot to overcontrol directionally while on the takeoff roll.

Care must be taken that traditional methods for checking linear servo-system performance, such as amplitude versus frequency and phase angle versus frequency, are not the sole criteria of acceptability. The practical approach is to observe the camera drive in operation, watching for lack of smoothness, especially at low rates.

Some visual system requirements for takeoff certification work are:

1. Accurate responsive camera motion drives, especially at low commanded rates, for prompt determination of engine failure without ambiguity. The camera drive must be "tight," having very little deadband or hysteresis.

2. A wide runway (300 feet) presentation with a well-defined center line and divider strips, preferably at 25-foot intervals, parallel to, and perpendicular to the center line. The lines parallel to the center line permit the pilot to estimate lateral deviations and the strips provide forward speed cues.

3. Accurate runway positioning so the pilot is able to use runway "distance remaining" markers as an indicator of location, and so that the end of the runway appears at the correct location.

In general, the quality of visual scene image required for takeoff is not so great as that required for studies involving landing approach and flare. However, there is the desirability of providing peripheral visual cues -- near-visual-field information for V_{MU} tests, far-field cues (horizon) for V_{MC_A} studies, and both for continuous take-off.

COCKPIT SOUND SIMULATION

A simple engine noise generator was installed and consisted of "white noise" plus a single frequency to represent engine "whine," both modulated in intensity according to the total thrust level.

Cockpit instrumentation provided the same 400 cps "whine" characteristic as the actual aircraft instruments which utilize 400 cps alternating current.

NONPILOTED PERFORMANCE RUNS

Much of the simulator performance was documented using the computer only. Typical of this procedure was the check of deceleration performance after a rejected takeoff. Nonpiloted runs were made (fig. 16) using average pilot recognition and reaction times taken from actual flight tests. Suitably biased comparator relays were used to make the engine fail at the desired speed, to cut remaining power, and to extend spoilers and apply brakes in rapid succession and with accurate timing.

INSTRUMENTATION NOTES

Care was taken to bias all annunciator and warning flags on primary flight instruments to the proper positions to avoid the possible consequences of a pilot becoming simulator conditioned (unintentionally, of course) to ignore the warning flag and later "chasing" an inoperative ILS needle or flight director during actual flight. For example, when the ILS glide slope needle was not in use the "OFF" flag would indicate the fact.

APPENDIX E

DYNAMIC EFFECTS ON MINIMUM UNSTICK SPEED

BACKGROUND

The determination of V_{MU} speed is accomplished by accelerating down the runway in the taxi attitude until shortly after $V_{1_{test}}$, when the elevator control is pulled full back and held until the aircraft begins to rotate. Elevator pressure is then relaxed to maintain the tail clearance corresponding to the angle of attack for $C_{L_{max}}$. When sufficient speed has been attained to provide lift greater than weight, lift-off will occur and V_{MU} is recorded.

Aircraft which, due to their geometrical shape, cannot be rotated to an angle of attack corresponding to $C_{L_{max}}$ with the main wheels still on the runway are said to be geometry limited. Several subsonic jet transports are so limited and were required (during certification) to demonstrate a geometry limited takeoff wherein the airplane was early rotated to the maximum possible angle of attack (by allowing the tail to strike and drag the ground) until sufficient speed was attained to permit lift-off. If the aircraft is not geometry limited, considerable pilot technique is required to rotate to and hold the proper tail clearance, especially at high thrust-to-weight ratios where lift-off occurs almost simultaneously with rotation. At the low T/W associated with V_{MU} for three engines, more time is available between rotation and lift-off to adjust tail clearance. Neither the visual scene nor the attitude indicator provided the sensitive cues required for precisely holding pitch attitude and so a tail clearance indicator (fig. 3), indicating from 5 feet to zero (tail contact), was provided and used as in the actual flight tests.

DYNAMIC EFFECTS

Dynamic effects associated with rapid elevator input at certain speeds can induce rotation and lift-off below V_{MU}. (Conventional V_{MU} is obtained using a steady-state elevator input until the airplane is rotating.) These dynamic effects are known to exist on several subsonic jet transports and are attributed to such terms as C_{m_q}, $C_{m_{\dot{\alpha}}}$, C_{L_q}, and $C_{L_{\dot{\alpha}}}$.

Wind-tunnel results from pitching and oscillating model tests yield the combined effects of pitch rate q and angle-of-attack rate $\dot{\alpha}$. Before these values are inserted into the simulator computer it is desirable to determine the relative proportions due to q and to $\dot{\alpha}$. Estimates from aerodynamicists ranged from 12:1 to 3:1, q being the larger. The present simulation neglected $C_{L_{\dot{\alpha}}}$. The figure below shows the results of a series of simulator takeoffs both piloted and computer-only involving step inputs of full elevator at progressively higher speeds and serves to illustrate the type of detailed research which may be accomplished.

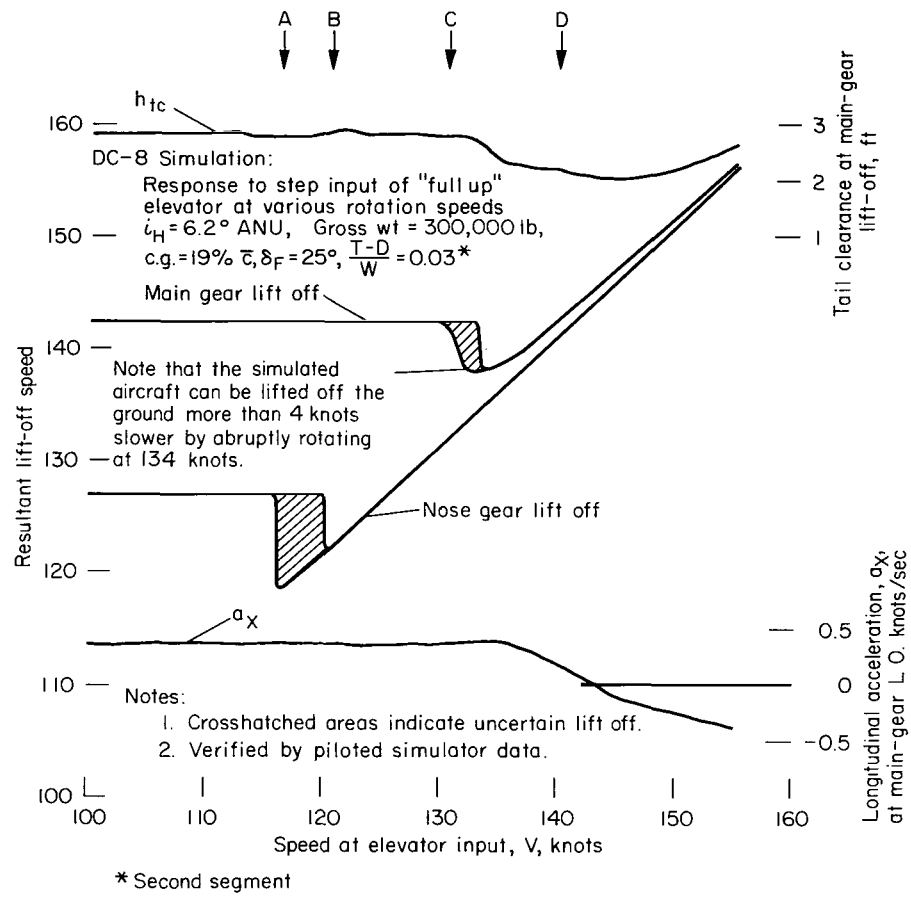

If full elevator is abruptly applied at any speed below A, the nose gear lifts off at 127 knots and the main gear at a V_{MU} of 142 knots; if between A and B, the nose wheel lifts off immediately, and then settles back to lift off a second time. If the rotation input is initiated at any speed between B and C, the nose wheel lifts off almost immediately, but the main gear still lifts off at 142 knots; however, if the control column is snapped back at speeds between C and D, the nose wheel lifts off the runway within one knot later and the main wheels lift off a few knots below the 142 knot V_{MU}. These same characteristics were demonstrated in the airplane.

Note that the bucket-shaped area formed in the curves covers a very narrow rotation speed range and a good portion involves momentary or uncertain lift-off. Even if lift-off is successful at speeds below V_{MU} the aircraft may not be capable of accelerating and climbing out of ground effect within the field length available.

Future programs could well utilize the simulator to study the relative contributions of the various dynamic terms as a function of piloting technique.

REFERENCES

1. Anon.: Airplane Airworthiness; Transport Categories. Civil Aeronautics Manual 4b, with amendments and supplements. Federal Aviation Agency, Sept. 1962 (replaced by Airworthiness Standards: Transport Category Airplanes. Part 25, Federal Air Regulations. Federal Aviation Agency, Feb. 1, 1965).

2. Anon.: Turbine-Powered Transport Category Airplane of Current Design. Special Civil Air Regulation SR-422B, Federal Aviation Agency, July 9, 1959.

3. Cooper, George E.: The Use of Piloted Flight Simulators in Take-Off and Landing Research. AGARD Rep. 430, Jan. 1963.

4. Bray, Richard S.: A Piloted Simulator Study of Longitudinal Handling Qualities of Supersonic Transports in the Landing Maneuver. NASA TN D-2251, 1964.

5. Barnes, A. G.: Simulator Assessments of Take-Off and Landing. AGARD Rep. 432, Jan. 1963.

6. Tymczyszyn, Joseph J.; and Spiess, Paul C.: The Effects of Supersonic Transport Flight Characteristics on Performance Requirements. Paper 674D SAE/ASNE, April 8-11, 1963.

7. Anon.: Estimated Aerodynamic Characteristics for Stability and Control Calculations, Model DC-8 Jet Transport. Rep. SM-19261, Douglas Aircraft Co., May 17, 1961.

8. Anon.: FAA Approved Airplane Flight Manual Model DC-8-21, 31, 32, and 33 (JT4). Rep. SM-23889 (with amendments), Douglas Aircraft Co., Jan. 1960.

9. Betts, G. L.: JT4 Engine Slotted Wing FAA Certification Tests: Aerodynamics. Model DC-8 Airplane, DEV-3203, Douglas Aircraft Co., vols. 1 and 2, Revision 13, August 20, 1961.

10. Walley, W. R.: DC-8 Performance to Show Compliance With Civil Air Regulations SR-422B; Pratt and Whitney JT4A-3, -5 Engines. Douglas Aircraft Co., revised August 4, 1962.

11. Reuselaars, D. J.; and Ahn, H. H. C.: Development of Stabilizer Setting for Takeoff, Model DC-8 With Leading Edge Slots. Rep. LB-31075, Douglas Aircraft Co., Nov. 1, 1962.

12. Salamacha, E. G.: Summary of Flight Test Data on the Dutch Roll Characteristics of the DC-8 With the Yaw Damper Inoperative. Company Memorandum CI-250-63-Aero-79, Douglas Aircraft Co., Feb. 25, 1963.

13. Walley, W. R.: Landing Stopping Performance of the DC-8 Under Various Conditions of Runway Surfaces. Paper presented at the DC-8 Hydraulic Symposium, Long Beach, Calif., Oct. 19, 1961.

14. Anon.: DC-8 Symposium: Aerodynamics. Douglas Aircraft Co., Oct. 19, 20, and 21, 1961.

15. Potts, James K.; and Fulton, Fitzhugh L., Jr.: B-58A Minimum Control Speed Test. FTC-TDR-63-29, Air Force Flight Test Center, Jan. 1964.

16. Connelly, Mark E.: Simulation of Aircraft. Tech. Rep. NAVTRADEVCEN 7591-R-1, U.S. Naval Training Device Center, Feb. 1958, reprinted May 1959.

17. Sellers, W. H.; and Caulkins, R. W.: Dynamics of Landing Gear Impact, Rebound, and Runout. WADD-TR-60-483, prepared by Fairchild Engine and Aircraft Corp., Hagerstown, Md., April 1962.

18. Dommasch, Daniel Otto; Sherby, Sydney S.; and Connolly, Thomas F.: Airplane Aerodynamics. Second ed., Pitman Publishing Corp., N. Y., 1957.

19. Anon.: The Long and Short of It. USAF Flying Safety, Oct. 1959, pp. 16-18.

20. Pike, E. C.: Coefficients of Friction. J. Roy. Aero. Soc., vol. 53, Dec. 1949, pp. 1085-1094.

21. Harben, D. A. J.: Take-Off and Landing -- Braking Problems. J. Roy. Aero. Soc., vol. 67, no. 633, Sept. 1963, pp. 581-584.

22. Horne, Walter B.; Stephenson, Bertrand H.; and Smiley, Robert F.: Low-Speed Yawed-Rolling and Some Other Elastic Characteristics of Two 56-Inch-Diameter, 24-Ply-Rating Aircraft Tires. NACA TN 3235, 1954.

23. Joyner, Upshur T.; Horne, Walter B.; and Leland, Trafford J. W.: Investigations on the Ground Performance of Aircraft Relating to Wet Runway Braking and Slush Drag. AGARD Report 429, Jan. 1963.

24. Smiley, Robert F.; and Horne, Walter B.: Mechanical Properties of Pneumatic Tires With Special Reference to Modern Aircraft Tires. NACA TN 4110, 1958.

25. Vickers-Armstrongs (Aircraft) Ltd.: Flight Tests to Determine the Coefficient of Friction Between an Aircraft Tyre and Various Wet Runway Surfaces; Part 9, Trials on an Asphalt Runway at Wisley. British Ministry of Aviation S & T Memo 17/62, Jan. 1963.

26. Clousing, Lawrence A.: Simulator Requirements Deduced From Comparisons of Pilot's Performance in Ground Simulators and in Aircraft. Presented at the 4th Congress of the International Council of Aeronautical Sciences, Paris, France, Aug. 24-28, 1964.

27. Sadoff, Melvin; and Harper, Charles W.: Piloted Flight Simulator Research. A Critical Review. Aero/Space Engineering, vol. 21, no. 9, Sept. 1962, pp. 50-63.

28. Weil, Joseph: Piloted Flight Simulation at the NASA Flight Research Center. Presented at IEEE 10th Annual East Coast Conf. on Aerospace and Navigational Electronics, Baltimore, Md., Oct. 21-23, 1963.

29. White, Maurice D.; Sadoff, Melvin; Bray, Richard S.; and Cooper, George E.: Assessment of Critical Problem Areas of the Supersonic Transport by Means of Piloted Simulators. Aero/Space Engineering, vol. 21, no. 5, May 1962, pp. 12-21.

30. Holleman, Euclid C.; and Wilson, Warren S.: Flight-Simulator Requirements for High-Performance Aircraft Based on X-15 Experience. Paper 63-AHGT-81, Am. Soc. Mech. Engrs., March 1963.

BIBLIOGRAPHY

Anon.: FAA Certification Tests for the Model DC-8 Airplane Equipped With P and W JT3D Engines. DEV-2712, Addendum No. 1, Douglas Aircraft Co., Dec. 27, 1960.

Anon.: Multiple V_1. The Air Line Pilot, June-July 1963, pp. 8-11, 22.

Buell, D. R.: Methods of Analysis of Performance of Commercial Turbojet Airplanes. DEV-2921, Douglas Aircraft Co., July 31, 1959.

Carbaugh, Carol C.; and Cross, Carl S.: KC-135A Heavyweight Three Engine Takeoff Performance Test. FTC-TDR-63-18, Air Force Flight Test Center, Dec. 18, 1963.

Cheney, H. K.: SST Flight Test Requirements for Certification of Take-Off/Landing Performance. Fifth Annual Symp. on Supersonic Transports, The Society of Experimental Test Pilots, Sept. 1961, pp. 175-199.

Crawford, Charles C.; and Gandy, Charles L., Jr.: ARDC KC-135A Heavy Weight Take-Off Performance Tests. TR-58-26, Addendum No. 1, Air Force Flight Test Center, Oct. 1958.

Crawford, Charles C.; and Seigler, Jones P.: ARDC KC-135A Stability and Control Test. TR-58-13, Air Force Flight Test Center, May 1958. ASTIA No. AD-152141.

Miles, E. C.: Take-Off and Landing Problems -- The Pilot's Point of View. J. Roy. Aero. Soc., vol. 67, no. 633, Sept. 1963, pp. 539-543.

O'Connor, J. J.: Generalized Curves for Aircraft Field Length Prediction Based on Analog Computer Simulation. Tech. Info. Series No. R61-SE87, General Electric, Aug. 11, 1961.

Overesch, E.: The Problems of Exact Calculation of Take-Off and Landing Characteristics of Conventional Transport Aircraft. AGARD Rep. 417, Jan. 1963.

Phillips, William H.: Appreciation and Prediction of Flying Qualities. NACA Rep. 927, 1949.

Spence, A.; and Lean, D.: Some Low-Speed Problems of High-Speed Aircraft. AGARD Rep. 357, April 1961.

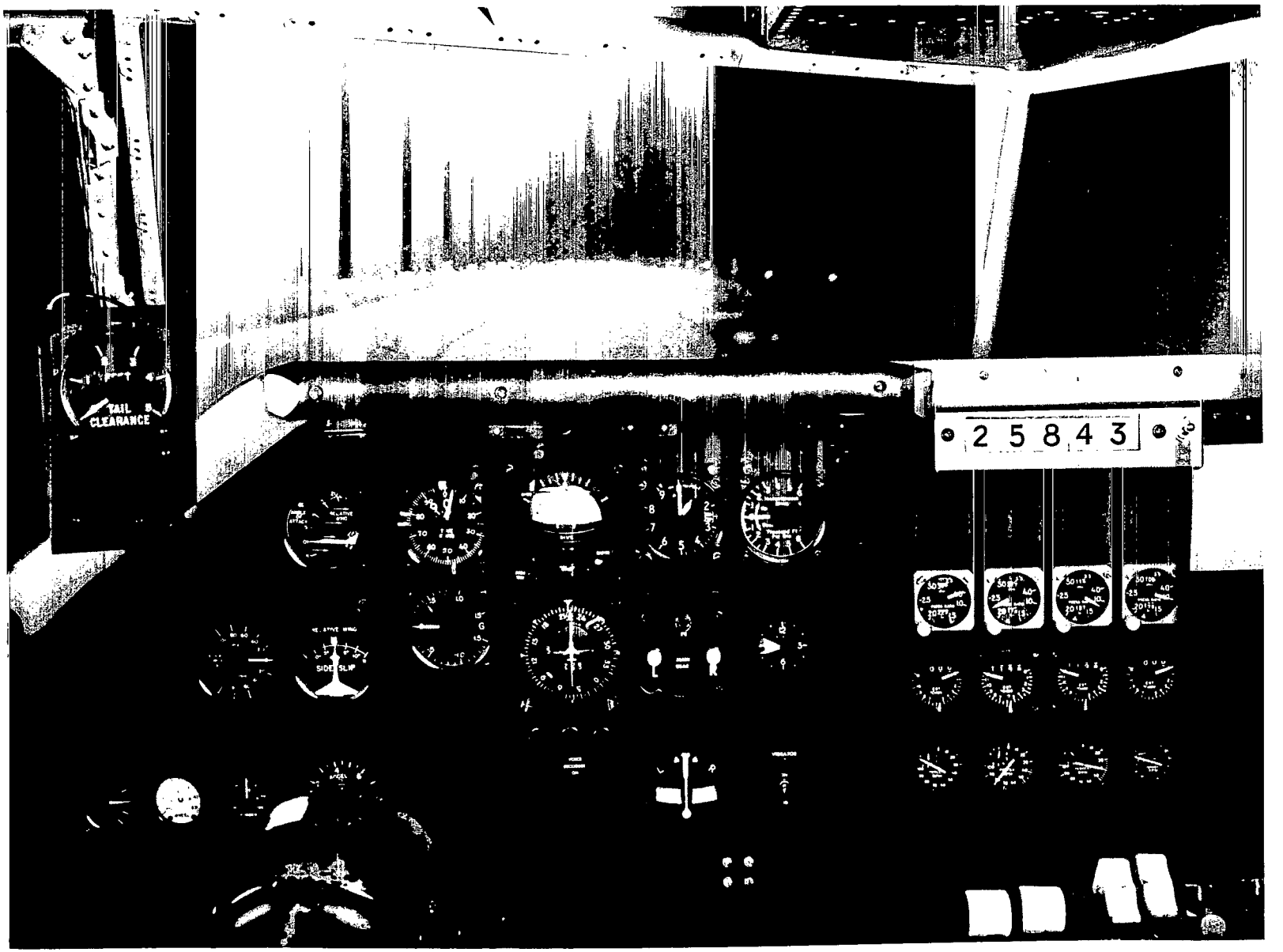

Figure 1.- Pilot's view of instrument display and runway in takeoff simulator. A-32752-5.3

A-32752-1

Figure 2.- One of the general purpose analog computers and the recording facilities utilized in takeoff simulation study.

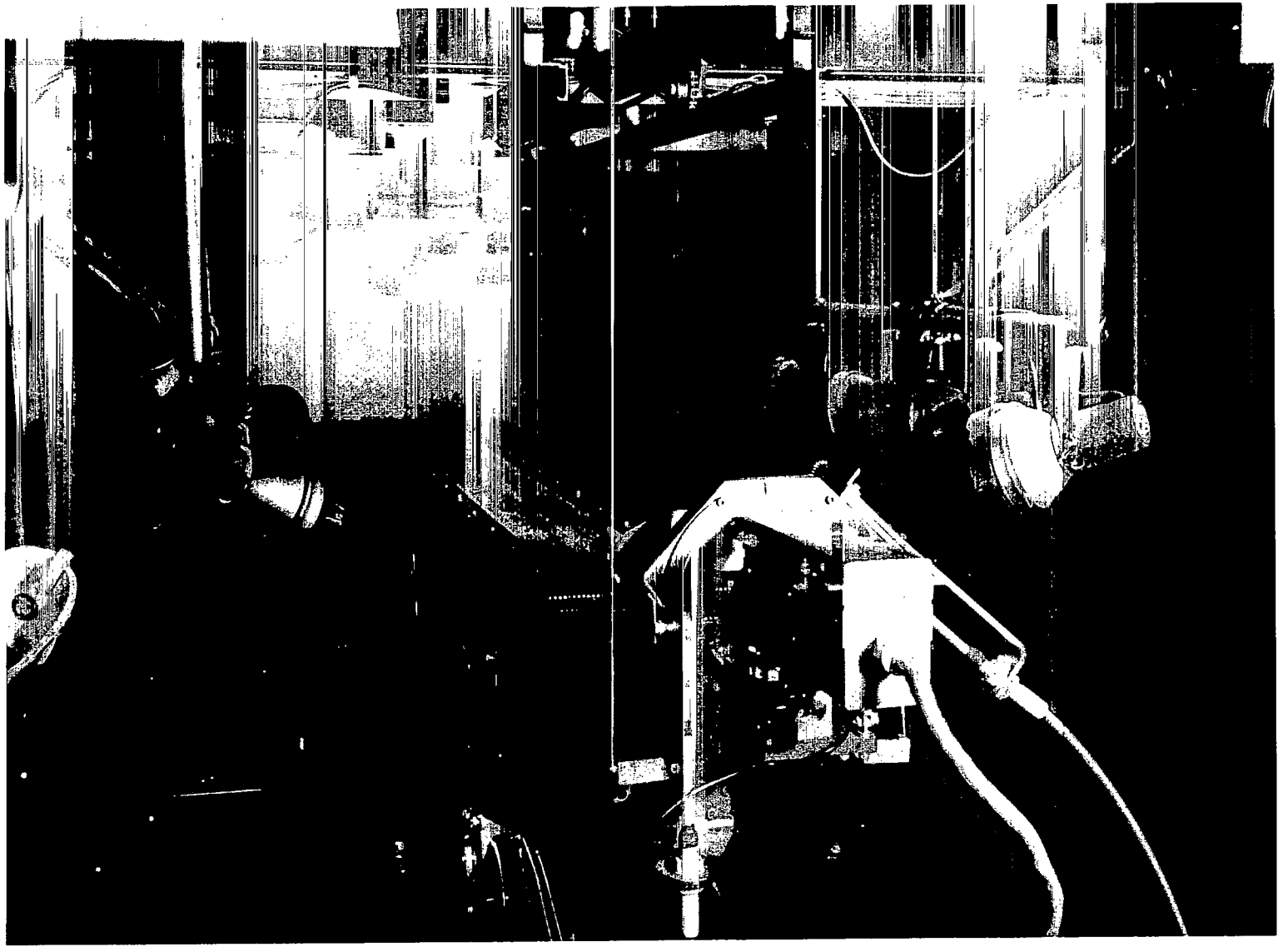

A-31062

Figure 3.- View of visual simulator showing servo-driven TV camera and model runway.

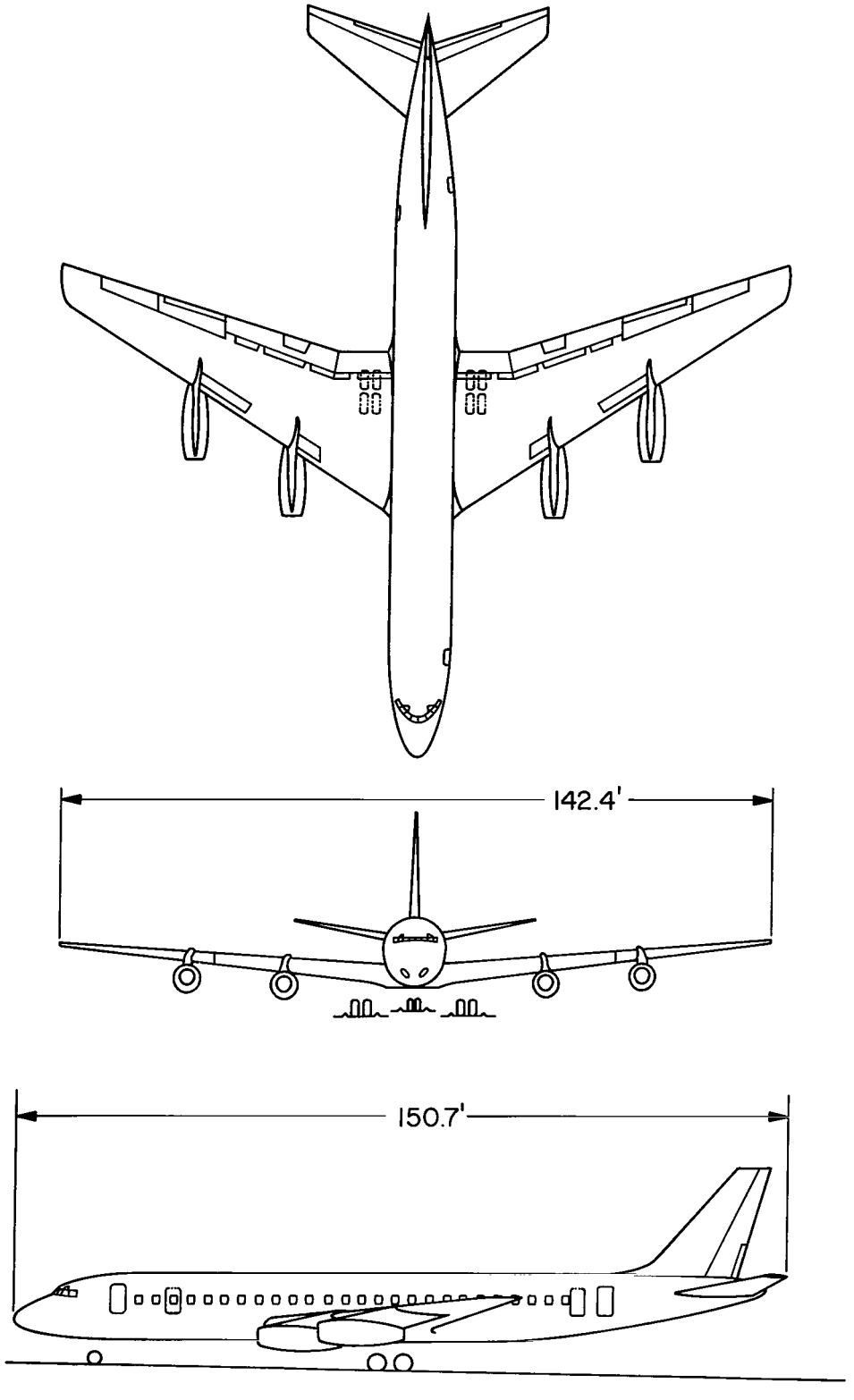

Figure 4.- Three-view drawing of test airplane.

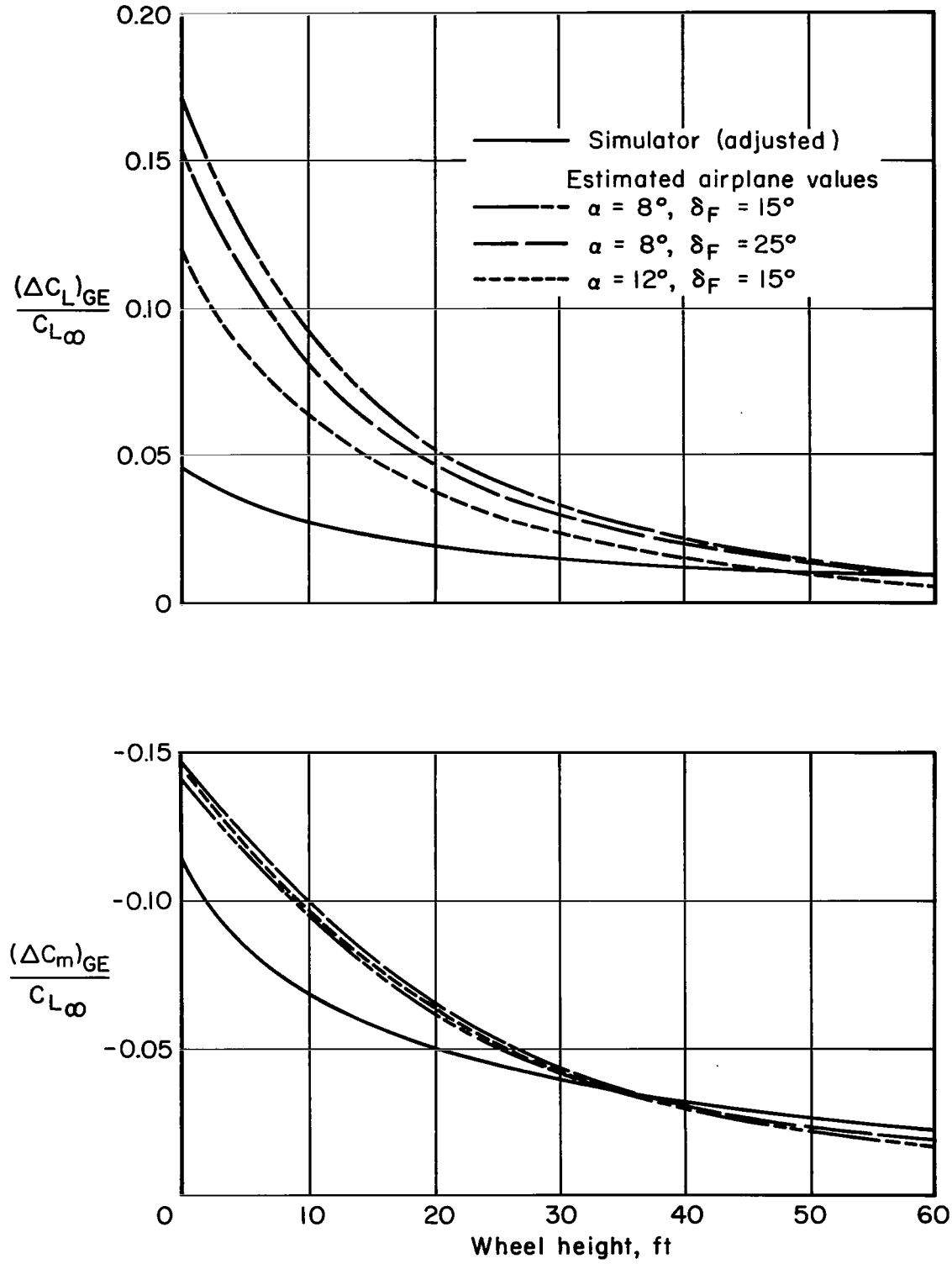

Figure 5.- Presence of ground plane influence on aerodynamic lift and pitching moment.

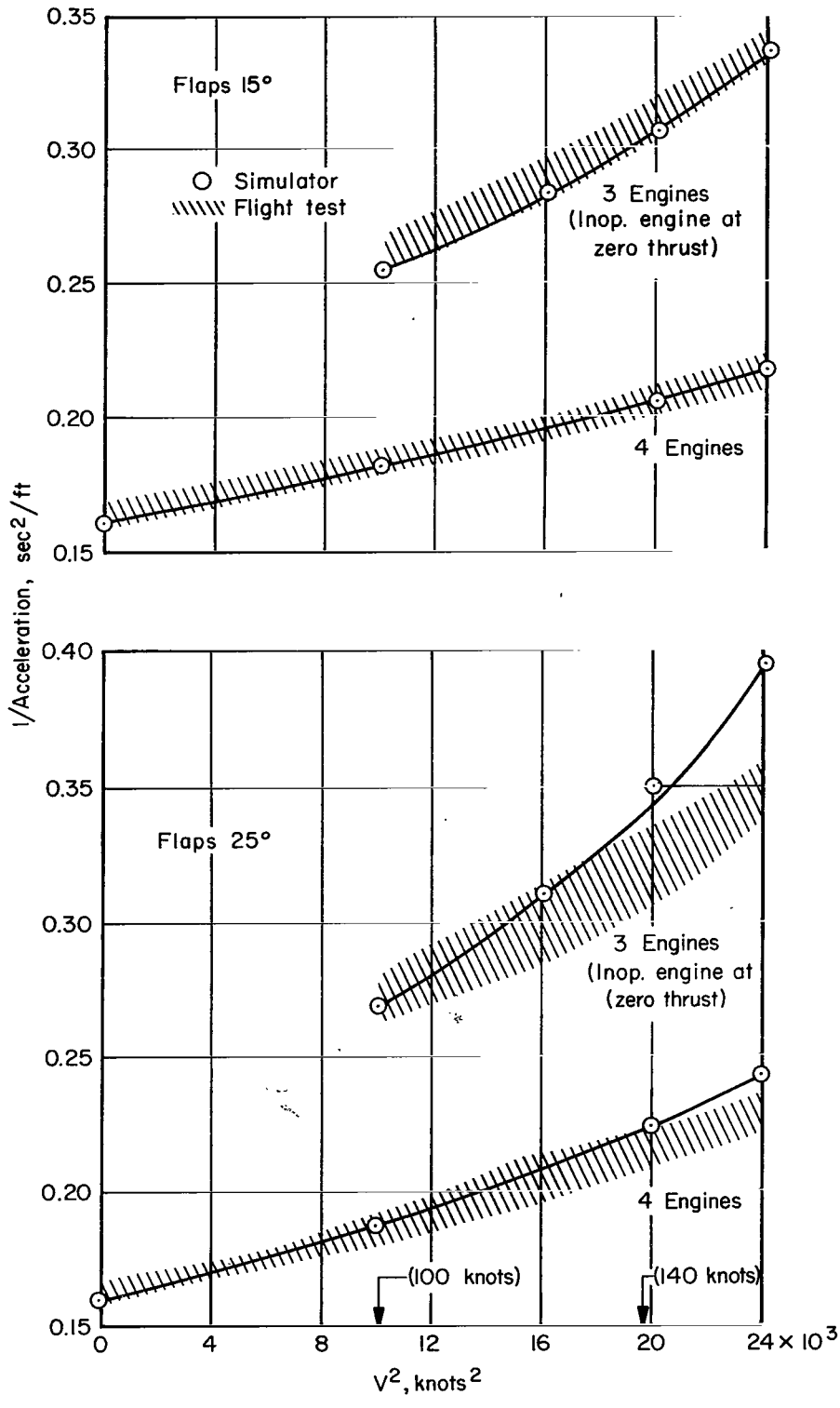

Figure 6.- Comparison of longitudinal accelerations in taxi attitude for simulator and flight test takeoffs; gross weight = 300,000 lb; JT4A-3 engines at takeoff thrust.

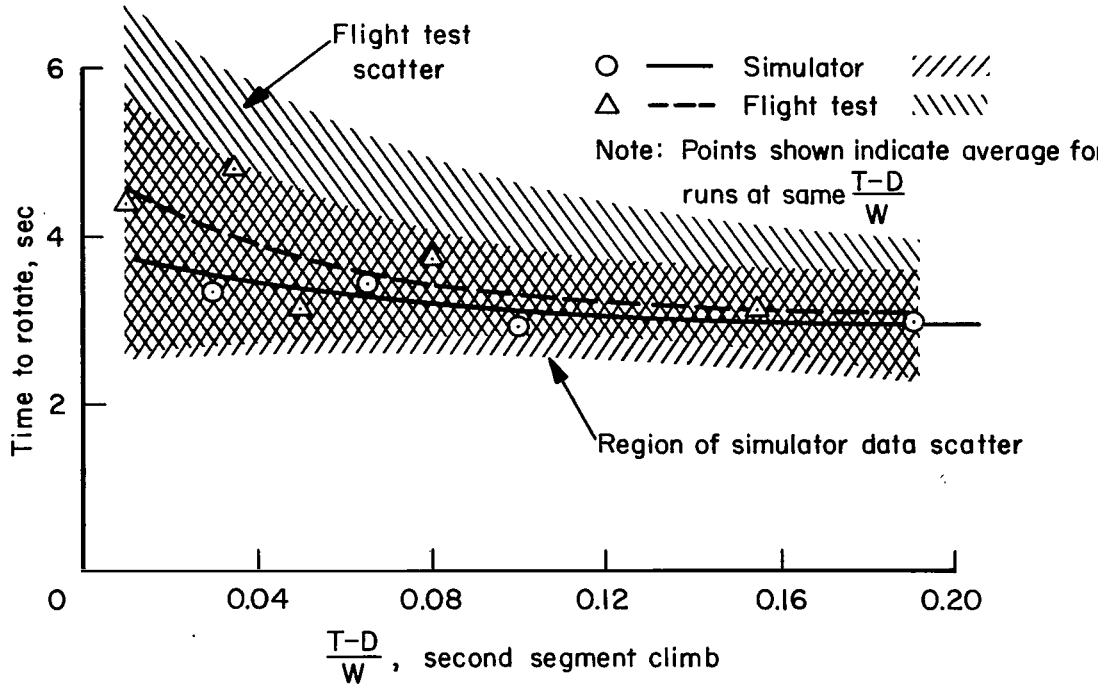

Figure 7.- Comparison of times from rotation initiation to lift-off for flight test and simulator takeoffs.

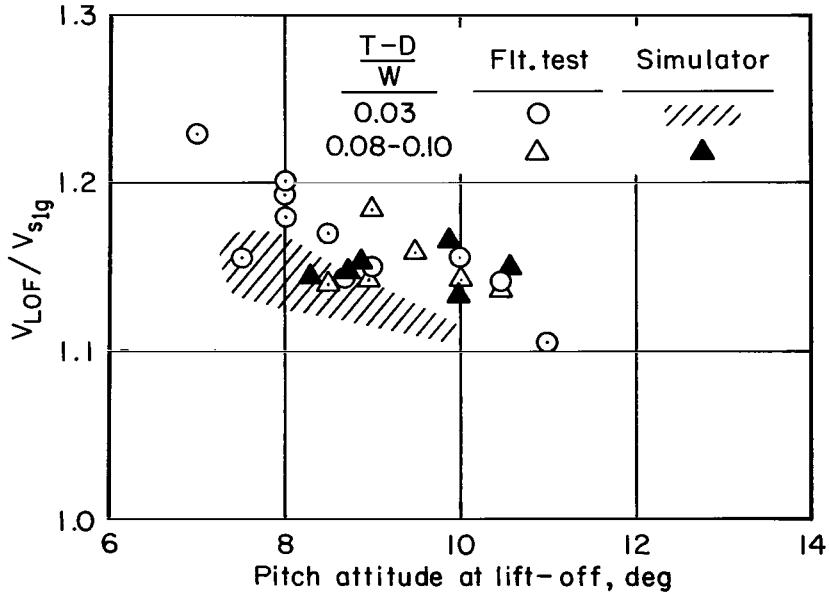

Figure 8.- Comparison of lift-off speed-pitch attitude relationship for flight test and simulator takeoffs.

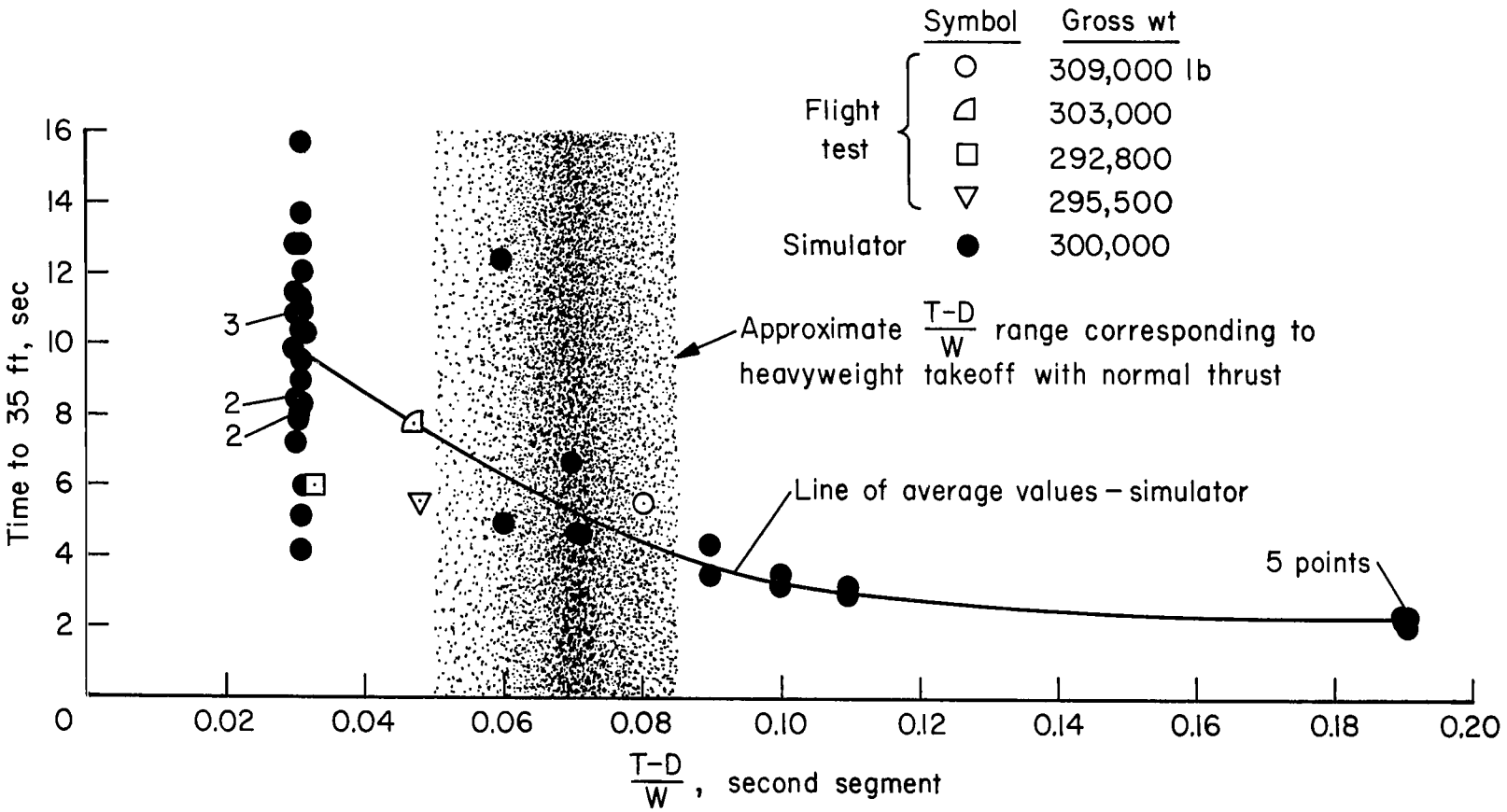

Figure 9.- Comparison of times from lift-off to 35-foot height for simulator and flight test takeoffs.

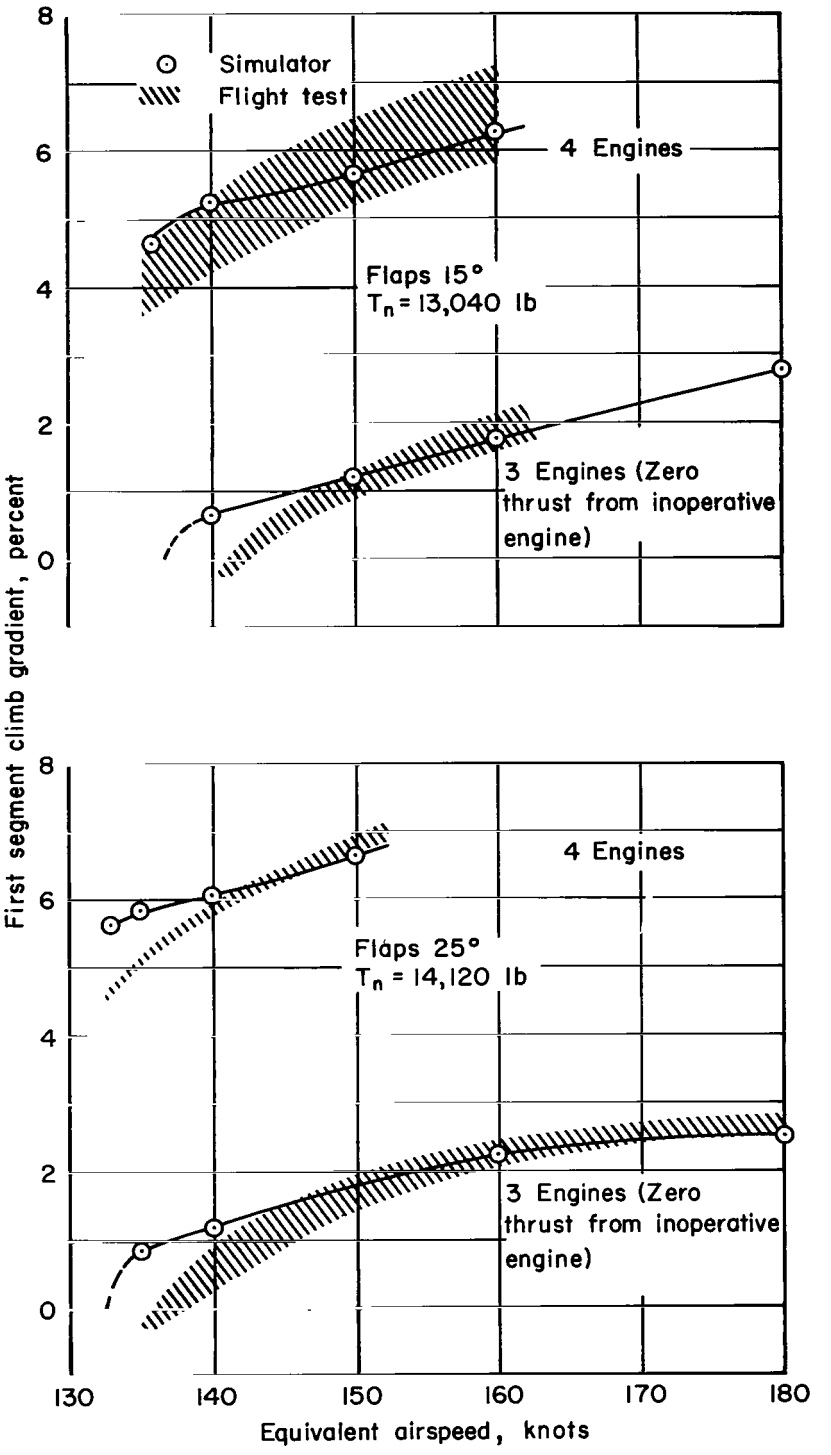

Figure 10.- First segment climb performance versus speed for flight test and simulator takeoffs; gross weight = 300,000 lb; gear extended; out of ground effect.

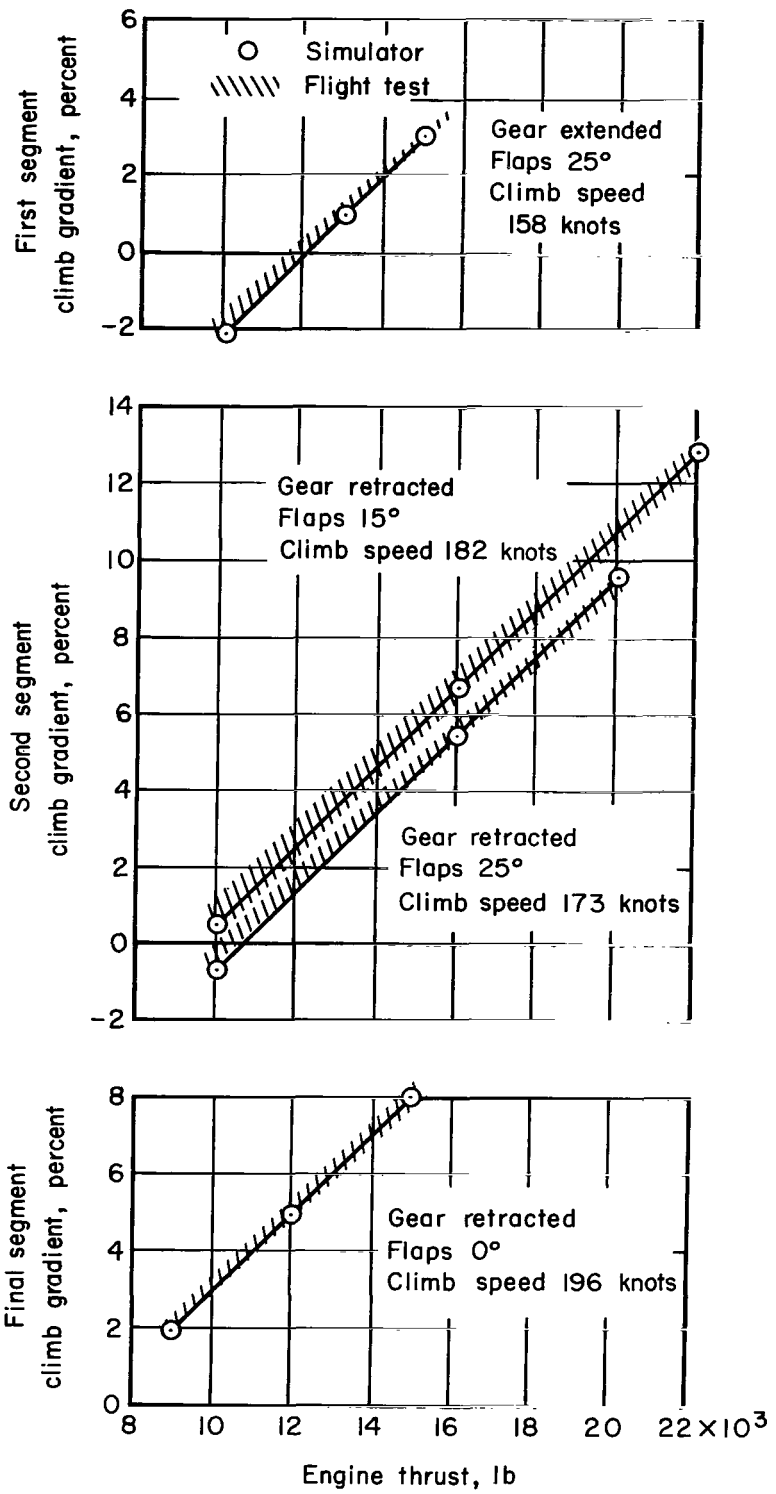

Figure 11.- Comparison of first, second, and final segment climb performances for flight test and simulator takeoffs; gross weight = 300,000 lb; three engines operative.

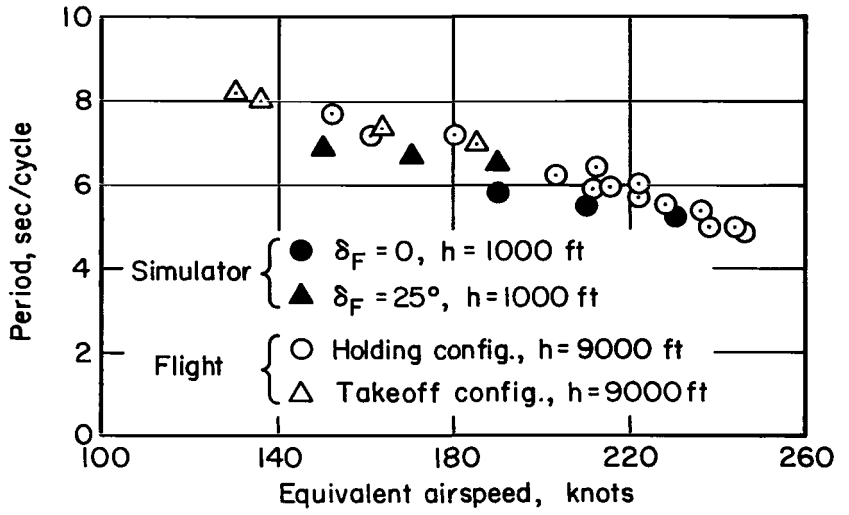

Figure 12.- Comparison of Dutch roll period from simulator and flight test investigations.

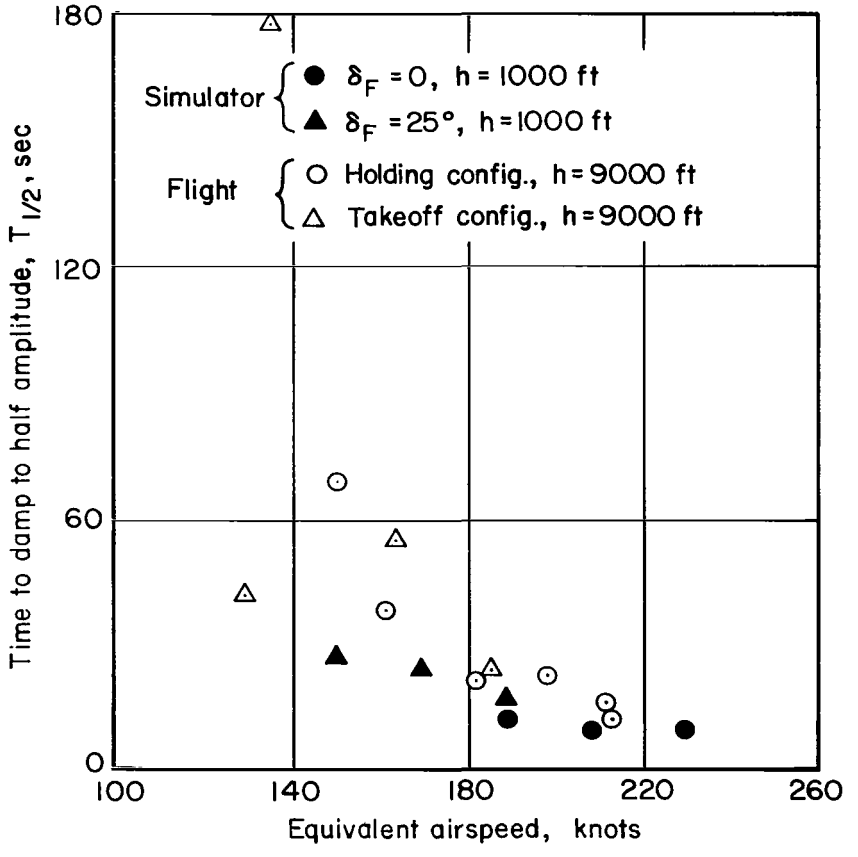

Figure 13.- Comparison of the times required to damp Dutch roll to one-half amplitude from simulator and flight test investigations.

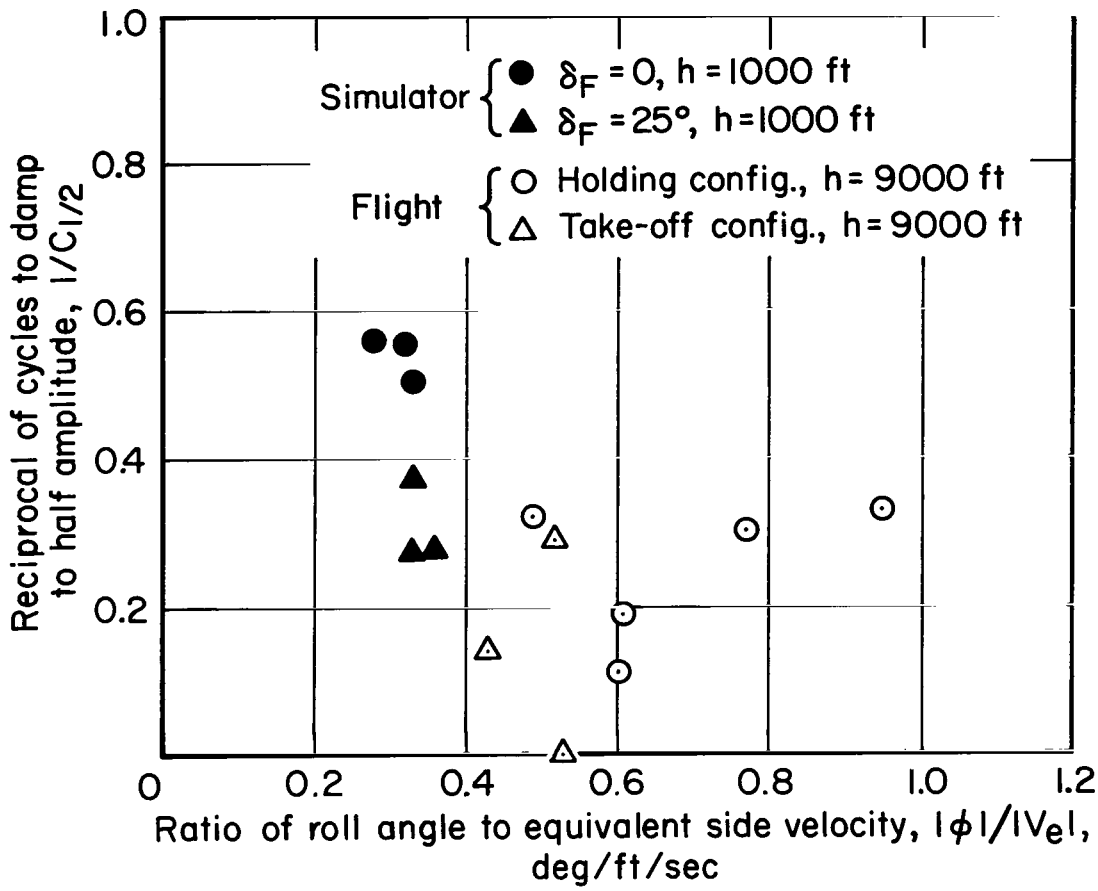

Figure 14.- Dutch roll parameters, $1/C_{1/2}$ versus $|\varphi|/|V_e|$ from simulator and flight test results.

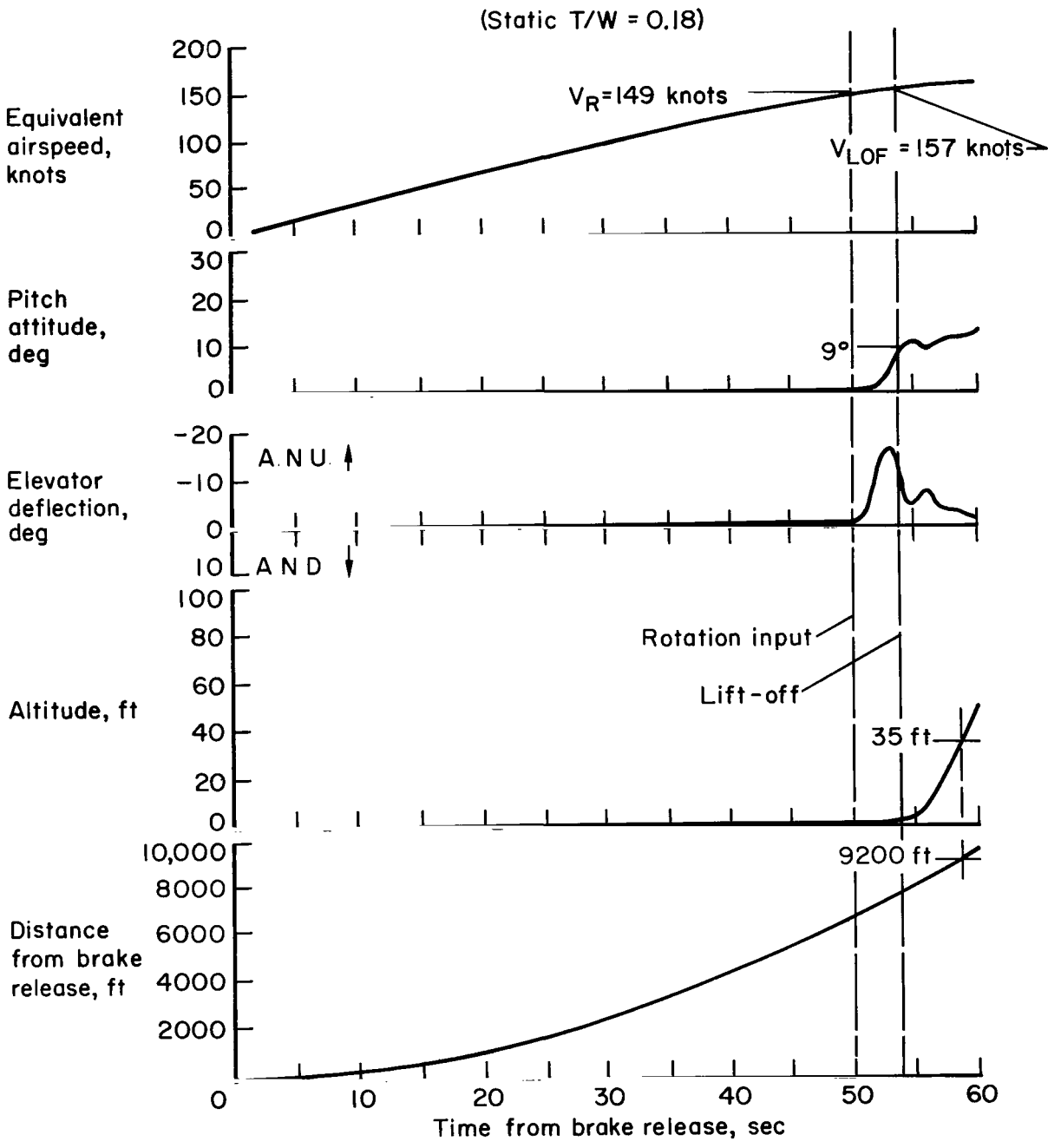

Figure 15.- Time history of a representative simulated takeoff; gross weight = 300,000 lb; static T/W = 0.18.

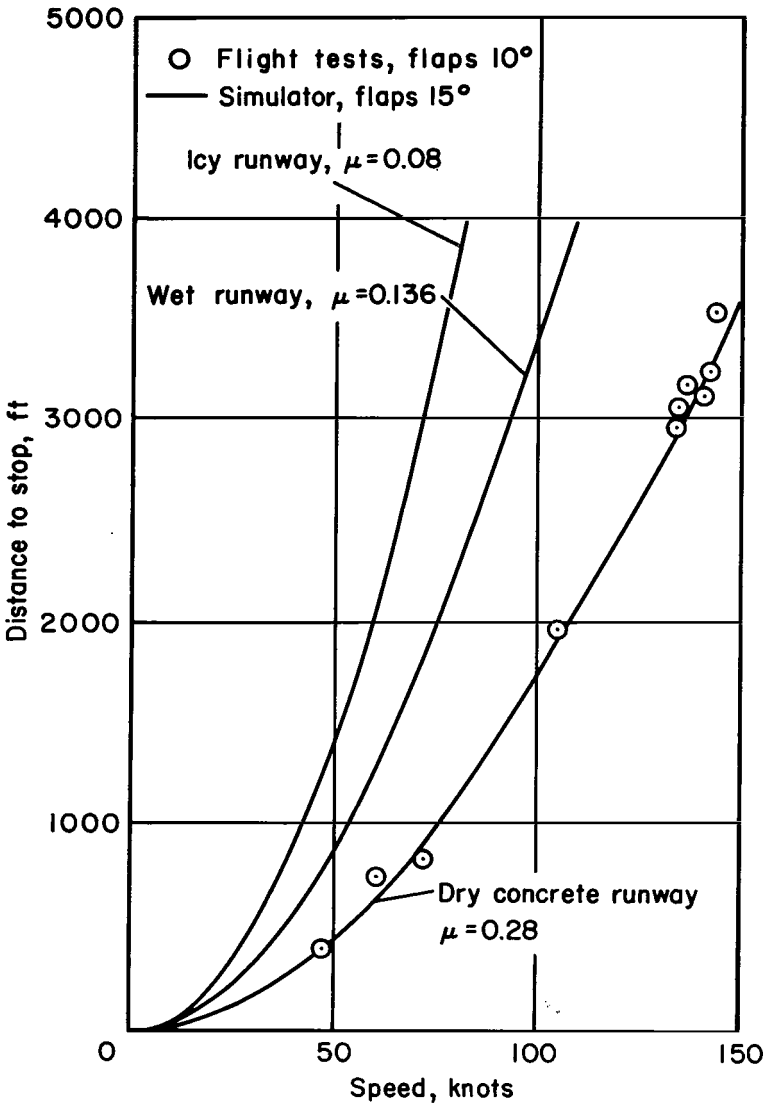

Figure 16.- Distance to stop following brake application during rejected takeoffs; gross weight = 300,000 lb.

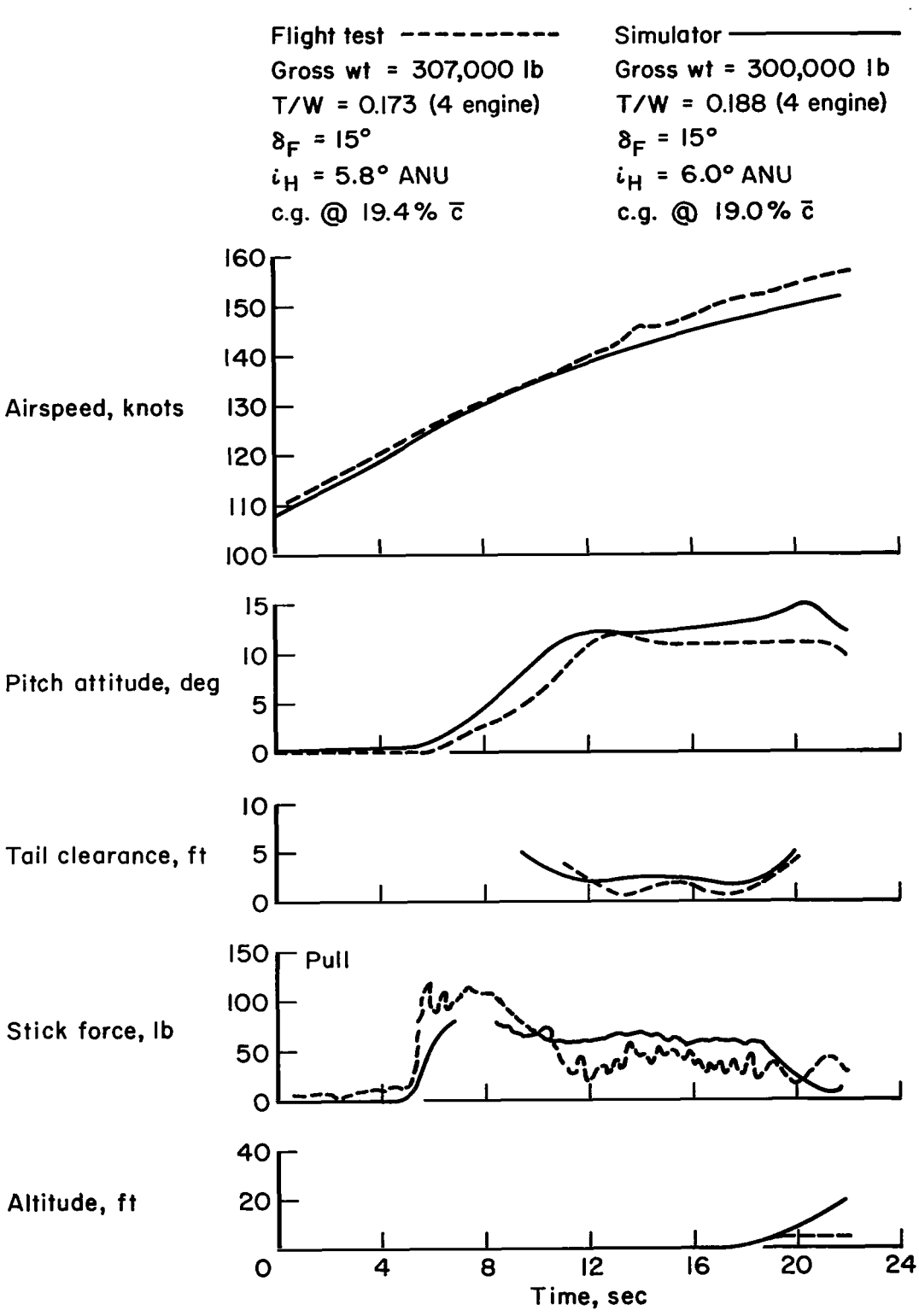

Figure 17.- Comparison of typical simulator and flight test V_{MU} takeoffs.

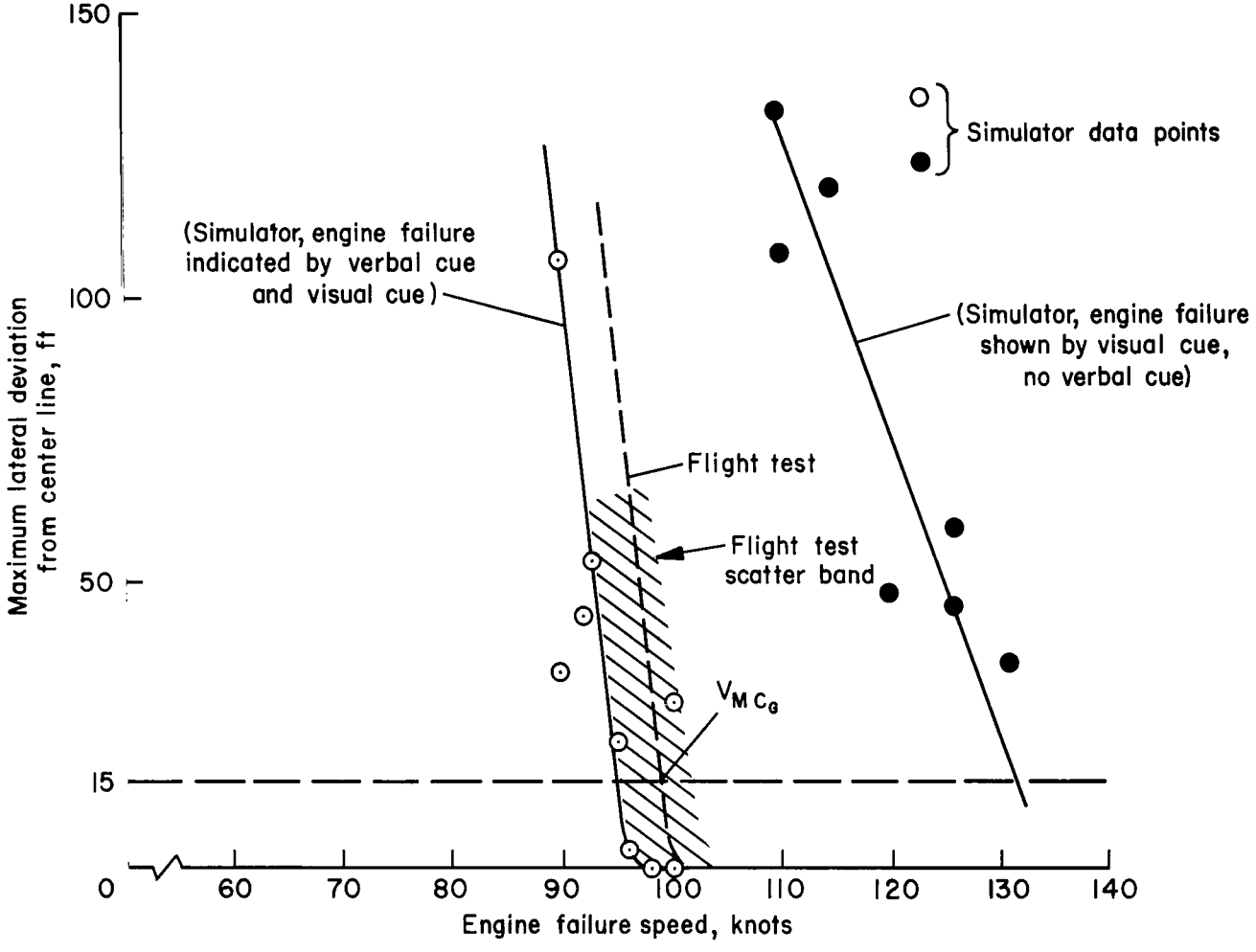

Figure 18.- Determination of ground minimum control speed; simulated gross weight = 200,000 lb; approximate flight test gross weight = 180,000 lb; c.g. = 32 percent $\bar{c}$; asymmetric thrust = 13,000 lb; JT4A-3 engines.

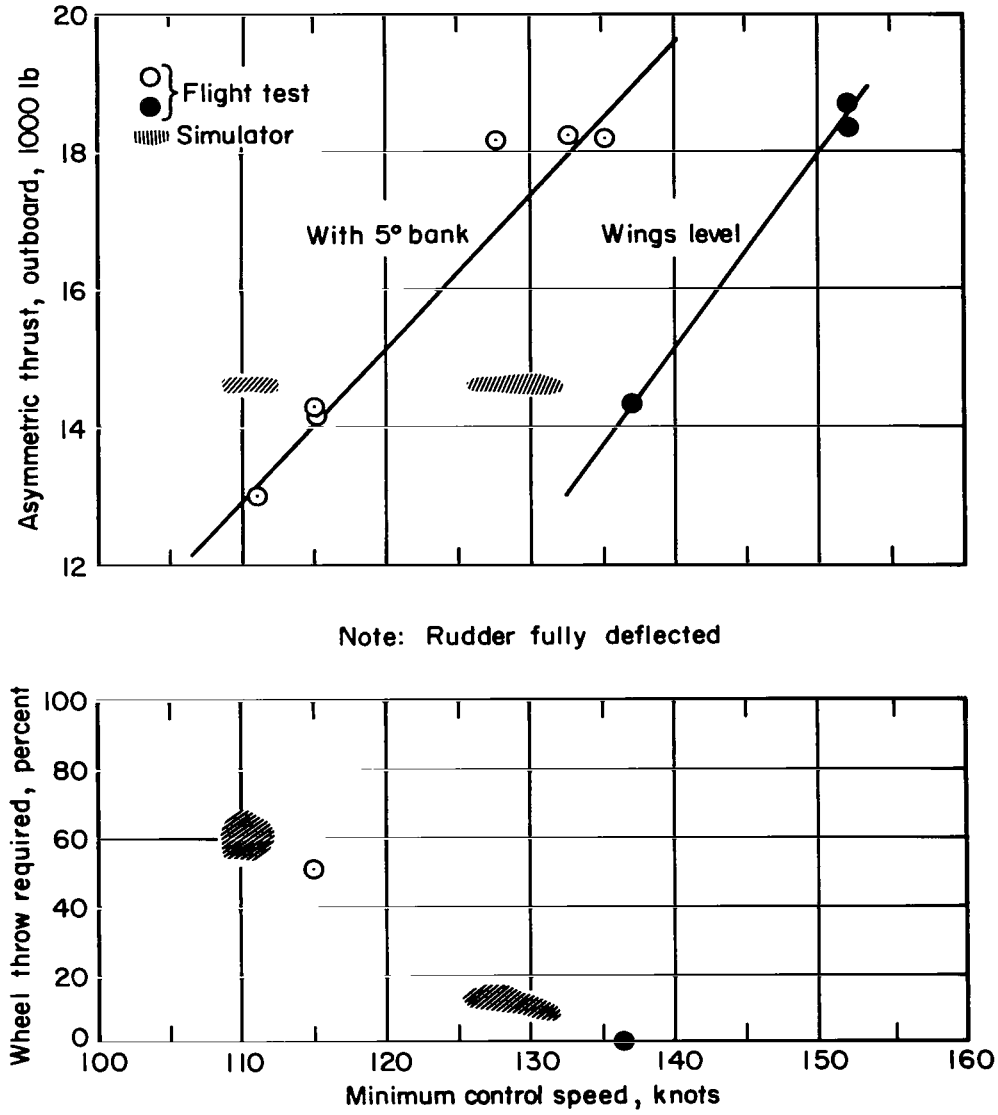

Figure 19.- Determination of air minimum control speed; simulated gross weight = 200,000 lb; flight test gross weight range = 147,000-202,000 lb; 25° flaps.

$$F_R = f(Z_R) + b_{mg}\dot{Z}_R \qquad F_R \geq 0,\ b_{mg}\dot{Z}_R = 0 \text{ when } Z_R \leq 0$$

$$Z_R = -h + y_{mg}\,\phi + (l_{mg} + l_{cg})\,\theta$$

$$\dot{Z}_R = -\dot{h} + y_{mg}\,p + (l_{mg} + l_{cg})\,q$$

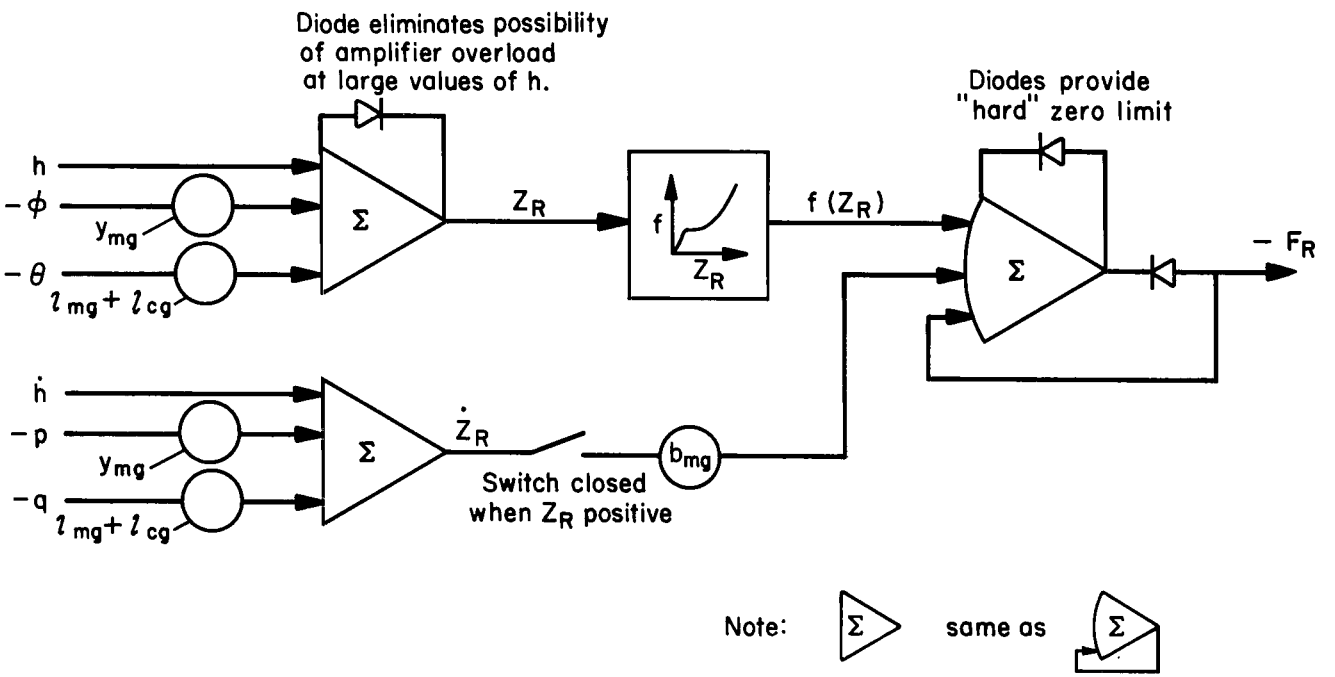

Figure 20.- Example of analog circuit for computation of landing-gear-reaction normal force.

"The aeronautical and space activities of the United States shall be conducted so as to contribute . . . to the expansion of human knowledge of phenomena in the atmosphere and space. The Administration shall provide for the widest practicable and appropriate dissemination of information concerning its activities and the results thereof."

—NATIONAL AERONAUTICS AND SPACE ACT OF 1958

NASA SCIENTIFIC AND TECHNICAL PUBLICATIONS

TECHNICAL REPORTS: Scientific and technical information considered important, complete, and a lasting contribution to existing knowledge.

TECHNICAL NOTES: Information less broad in scope but nevertheless of importance as a contribution to existing knowledge.

TECHNICAL MEMORANDUMS: Information receiving limited distribution because of preliminary data, security classification, or other reasons.

CONTRACTOR REPORTS: Technical information generated in connection with a NASA contract or grant and released under NASA auspices.

TECHNICAL TRANSLATIONS: Information published in a foreign language considered to merit NASA distribution in English.

TECHNICAL REPRINTS: Information derived from NASA activities and initially published in the form of journal articles.

SPECIAL PUBLICATIONS: Information derived from or of value to NASA activities but not necessarily reporting the results of individual NASA-programmed scientific efforts. Publications include conference proceedings, monographs, data compilations, handbooks, sourcebooks, and special bibliographies.

Details on the availability of these publications may be obtained from:

SCIENTIFIC AND TECHNICAL INFORMATION DIVISION

NATIONAL AERONAUTICS AND SPACE ADMINISTRATION

Washington, D.C. 20546